Neurobiology of Disease 190 (2024) 106388

Contents lists available at ScienceDirect

Neurobiology of Disease

journal homepage: www.elsevier.com/locate/ynbdi

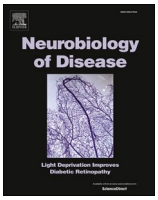

Megalencephalic leukoencephalopathy with subcortical cysts protein-1: A new calcium-sensitive protein functionally activated by endoplasmic reticulum calcium release and calmodulin binding in astrocytes

M.S. Brignone [a,1], A. Lanciotti [a,1], P. Molinari [b], C. Mallozzi [a], C. De Nuccio [c], E.S. Caprini [a], T.C. Petrucci [a], S. Visentin [b,2], E. Ambrosini [a,*,2]

[a] Istituto Superiore di Sanità, Department of Neuroscience, Viale Regina Elena 299, 00161 Rome, Italy
[b] Istituto Superiore di Sanità, National Center for Drug Research and Evaluation, Viale Regina Elena 299, 00161 Rome, Italy
[c] Istituto Superiore di Sanità, Research Coordination and Support Service, Viale Regina Elena 299, 00161 Rome, Italy

ARTICLE INFO

Keywords:
CaM
CaMKII
ER Ca^{2+} release
CCE
Leukodystrophy
Rare diseases
Astrogliosis
VRAC
Regulatory volume decrease
EGFR

ABSTRACT

Background: MLC1 is a membrane protein highly expressed in brain perivascular astrocytes and whose mutations account for the rare leukodystrophy (LD) megalencephalic leukoencephalopathy with subcortical cysts disease (MLC). MLC is characterized by macrocephaly, brain edema and cysts, myelin vacuolation and astrocyte swelling which cause cognitive and motor dysfunctions and epilepsy. In cultured astrocytes, lack of functional MLC1 disturbs cell volume regulation by affecting anion channel (VRAC) currents and the consequent regulatory volume decrease (RVD) occurring in response to osmotic changes. Moreover, MLC1 represses intracellular signaling molecules (EGFR, ERK1/2, NF-kB) inducing astrocyte activation and swelling following brain insults. Nevertheless, to date, MLC1 proper function and MLC molecular pathogenesis are still elusive. We recently reported that in astrocytes MLC1 phosphorylation by the Ca^{2+}/Calmodulin-dependent kinase II (CaMKII) in response to intracellular Ca^{2+} release potentiates MLC1 activation of VRAC. These results highlighted the importance of Ca^{2+} signaling in the regulation of MLC1 functions, prompting us to further investigate the relationships between intracellular Ca^{2+} and MLC1 properties.

Methods: We used U251 astrocytoma cells stably expressing wild-type (WT) or mutated MLC1, primary mouse astrocytes and mouse brain tissue, and applied biochemistry, molecular biology, video imaging and electrophysiology techniques.

Results: We revealed that WT but not mutant MLC1 oligomerization and trafficking to the astrocyte plasma membrane is favored by Ca^{2+} release from endoplasmic reticulum (ER) but not by capacitive Ca^{2+} entry in response to ER depletion. We also clarified the molecular events underlining MLC1 response to cytoplasmic Ca^{2+} increase, demonstrating that, following Ca^{2+} release, MLC1 binds the Ca^{2+} effector protein calmodulin (CaM) at the carboxyl terminal where a CaM binding sequence was identified. Using a CaM inhibitor and generating U251 cells expressing MLC1 with CaM binding site mutations, we found that CaM regulates MLC1 assembly, trafficking and function, being RVD and MLC-linked signaling molecules abnormally regulated in these latter cells.

Abbreviations: MLC, Megalencephalic leukoencephalopathy with subcortical cysts; MLC1, Megalencephalic leukoencephalopathy with subcortical cysts protein-1; Ca^{2+}, Calcium; LD, Leukodystrophy; RVD, Regulatory volume decrease; VRAC, Volume regulated anion channel; $I_{Cl,swell}$, Swelling-activated Cl^- currents; ER, Endoplasmic reticulum; CICR, Calcium-induced calcium release; CaM, Calmodulin; CaMKII, Ca^{2+}/Calmodulin activated kinase; CNS, Central nervous system; SF, Serum-free conditions; CCE, Capacitative calcium entry; CMZ, Calmidazolium; TRPV4, Transient receptor potential vanilloid-4; EGFR, Epidermal growth factor receptor; GPRC5B, G Protein-Coupled Receptor Class C Group 5 Member B; AQP4, Aquaporin-4; aa, Amino acids; InsP3, Inositol 1,4,5-trisphosphate; DGC, Dystrophin/dystroglycan protein complex; KCNE, Potassium voltage-gated channel subfamily E member 1; ERK, Extracellular signal-regulated kinases 1/2; NF-kB, Nuclear factor kappa-light-chain-enhancer of activated B cells; STAT3, Signal transducer and activator of transcription 3; PLCγ, Phospholipase C, gamma 1; mGluR5, Metabotropic glutamate receptor 5; GFAP, Glial fibrillary acidic protein; Kir2.1, Inward-rectifier potassium channel 2.1; KCa3.1, Calcium-activated potassium channel 3.1..

* Corresponding author.
E-mail address: elena.ambrosini@iss.it (E. Ambrosini).
[1] These authors equally contributed to this work.
[2] Senior authors.

https://doi.org/10.1016/j.nbd.2023.106388
Received 23 June 2023; Received in revised form 4 December 2023; Accepted 18 December 2023
Available online 22 December 2023

Conclusion: Overall, we qualified MLC1 as a Ca^{2+} sensitive protein involved in the control of volume changes in response to ER Ca^{2+} release and astrocyte activation. These findings provide new insights for the comprehension of the molecular mechanisms responsible for the myelin degeneration occurring in MLC and other LD where astrocytes have a primary role in the pathological process.

1. Introduction

MLC1 is a 377-amino acid membrane protein with eight predicted transmembrane domains and short cytoplasmic amino and carboxylic tails showing very low similarity with some ion channels (Brignone et al., 2015; Bosch and Estévez, 2020). MLC1 is prominently expressed in brain astrocyte end-feet contacting blood vessels and meninges, and in the Bergmann glia of the cerebellum (Teijido et al., 2004; Boor et al., 2005; Ambrosini et al., 2008). Genetic mutations affecting different regions of the MLC1 protein cause megalencephalic leukoencephalopathy with subcortical cysts disease (MLC) (Leegwater et al., 2001), a rare congenital leukodystrophy (LD) where a primary astrocyte defect causes macrocephaly, ataxia, spasticity and progressive deterioration of motor and mental functions (Van der Knaap et al., 1996). MLC patients often suffer from epileptic seizures and their symptoms can worsen after minor head trauma or common infections (Hamilton et al., 2018). Magnetic resonance imaging (MRI) of MLC brain shows diffuse white matter edema and the presence of subcortical cysts (Van der Knaap et al., 1996; Hamilton et al., 2018). The examination of some tissue biopsies revealed myelin vacuolation and some degrees of astrogliosis (Van der Knaap et al., 1996; Pascual-Castroviejo et al., 2005; Duarri et al., 2011). Mutations in the *MLC1* gene are responsible for the disease in 75–80% of patients (Topçu et al., 2000; Leegwater et al., 2001), while in the others 15–20% mutations have been found in GlialCAM, a protein chaperoning MLC1 to the plasma membrane (PM), (López-Hernández et al., 2011; Capdevila-Nortes et al., 2013). Very recently, MLC disease has been associated to mutations in other two genes encoding the water channel aquaporin-4 (AQP4) and the G Protein-Coupled Receptor Class C Group 5 Member B (GPRC5B), both of which showed colocalization with MLC1/GlialCAM at astrocyte end-feet and functional relationships with the MLC1 protein complex (Passchier et al., 2023). Cellular and animal models indicated that lack of functional MLC1 affects the activation of the volume-regulated anion channel (VRAC) and regulatory volume decrease (RVD) in astrocytes in response to osmotic changes (Ridder et al., 2011; Hoegg-Beiler et al., 2014; Bugiani et al., 2017; Elorza-Vidal et al., 2018; Brignone et al., 2022). These experimental observations, along with the main clinical signs characterizing MLC brain (edema, fluid cysts, astrocyte vacuolation/swelling), suggest that defects in the MLC1-mediated control of astrocyte osmoregulation processes are responsible for myelin degeneration in this disease. In addition, normal, but not mutated MLC1, is capable to downregulate specific intracellular signaling pathways (including EGFR, ERK, PLC-γ, NF-kB and STAT3 molecules) activated in astrocytes by inflammatory, oxidative and osmotic stress signals (Lanciotti et al., 2016; Elorza-Vidal et al., 2018; Brignone et al., 2011, 2019). Accordingly, increased MLC1 expression has been reported in perivascular astrocytes in the brain of patients affected by degenerative and inflammatory diseases of the central nervous system (CNS), (Brignone et al., 2011, 2019). These results lead to suppose that MLC1 mutations cause abnormally reactive, hypertrophic astrocytes unable to rescue normal cell volume following changes in ion concentrations occurring physiologically throughout neuronal activity or pathologically in response to brain damage (Walch and Fiacco, 2022). Despite all these studies demonstrated the significant role played by MLC1 in astrocyte physiopathology, MLC1 proper function is still elusive. We previously found that MLC1 contributes to Ca^{2+} influx in astrocytes during osmotic stress (Lanciotti et al., 2012); in addition, defects in intracellular Ca^{2+} homeostasis were observed in some MLC pathological models (Petrini et al., 2013; Lanciotti et al., 2016). Interestingly, we recently reported that MLC1 phosphorylation by CaMKII in response to calcium release potentiates VRAC currents and confers calcium sensitivity to this channel in U251 astrocytoma cells (Brignone et al., 2022). Overall, these findings hint at a reciprocal relationship between astrocyte Ca^{2+} dynamics and MLC1 functions that deserves further investigations. The results here presented allow us to increase the knowledge on MLC1/Ca^{2+} signaling and on the molecular events governing astrocyte reactivity and swelling and whose deregulation may account for myelin vacuolation and edema in MLC brain.

2. Materials and methods

2.1. Cell cultures and treatments

Astrocyte-enriched cultures were generated from newborn CD1 Swiss mice (purchased from Harlan Laboratories, San Pietro al Natisone, Udine, Italy) and maintained in culture as previously described (Ambrosini et al., 2003; Eleuteri et al., 2017). Brain tissue samples were obtained from the same newborn animals. All the animal procedures are carried out in accordance with the European Communities Council Directive N. 2010/63/EU and using the procedure approved by the Ministry of Health (authorization number: 271/SSA/2010).

The U251 multiform glioblastoma (MG) cell line was kindly provided by Dr. A. Calogero and obtained from the ACCT collection (Calogero et al., 2004). U251 cell lines expressing recombinant MLC1 wild type (WT), mutated MLC1 (S280L) and the K^+ channel Kir2.1 and generated as previously described (Lanciotti et al., 2012), were grown in Dulbecco's modified Eagle's medium high glucose (DMEM, Euroclone, Ltd., UK), supplemented with 10% FBS (Gibco BRL, Paisley, UK), 1% penicillin/streptomycin (Euroclone) and 600 μg/ml of Geneticin G-418 (Sigma-Aldrich, Saint Louis, USA) for selection at 37 °C in a 5% CO_2/95% air atmosphere. For treatments, cells were plated in serum-free (SF) medium and stimulated for 5 or 15 min (min) with different concentrations of thapsigargin (TG, 100 nM, Santa Cruz Biotechnology, Inc., Santa Cruz, California), adenosine triphosphate (ATP, 100 μM, Sigma-Aldrich) and Lanthanum chloride ($LaCl_3$, 100 μM, Sigma-Aldrich). For hyposmotic stimulation, cells were treated for 15 min with isotonic solution (140 mM NaCl, 5 mM KCl, 2 mM $MgCl_2$, 2 mM $CaCl_2$, 20 mM D-glucose, 5 mM HEPES, pH 7.4) or with a hypotonic solution prepared by adding 40% distilled water to the isotonic solution (Hypo, in Ca^{2+}-free conditions or with 2 mM $CaCl_2$), as previously described (Brignone et al., 2022). To inhibit the interaction of CaM with MLC1, U251 MLC1-WT cells were pre-treated for 15 min with 1 μM Calmidazolium, a specific CaM inhibitor (CMZ, Calbiochem, San Diego, CA), in isotonic solution or SF DMEM, then co-stimulated for further 15 min in hypotonic solution or 5 min with ATP 100 μM in SF DMEM medium.

2.2. Generation of U251 cells expressing MLC1 with Calmodulin-binding site mutations

The construct encoding the MLC1 protein with mutations in the CaM binding motif was generated by site-directed mutagenesis of I324 and Q325 amino acid residues present in the putative CaM binding site of the human MLC1 sequence. The double mutation MLC1-IQ/AG was introduced by PCR using mismatched primers, amplifying the region between BamHI restriction site and the 3′-end of MLC1 coding sequence. The PCR products were used to replace the corresponding fragment of MLC1 WT sequence cloned into the retroviral expression vector pQCXIN (pQCXIN, Takara Bio Europe Clontech). The introduced mutations were confirmed by sequencing. Stable U251 line generation expressing the MLC1 mutant

was obtained as previously described (Lanciotti et al., 2012).

2.3. Immunofluorescence staining (IF) and fluorescence microscopy analysis

U251 cells expressing MLC1-WT were grown on polylysine (PLL)-coated coverslips and left untreated or treated with different doses of TG and ATP or with hyposmotic solution in the presence or not of CMZ (see above concentrations and time of stimulation) and used for IF staining. After treatments, cells were fixed for 10 min with 4% paraformaldehyde (PFA) and washed with phosphate-buffered saline (PBS). After 1 h of incubation with blocking solution (5% BSA in PBS), cells were incubated for 1 h at room temperature (RT) with the following primary antibodies (Abs) diluted in PBS containing 0.025% Triton X-100: anti-MLC1 polyclonal Ab (pAb) (1:50, Atlas AB, AlbaNova University Center, Stockholm, Sweden) and anti-CaM pAb (1:50, Santa Cruz Biotechnology). Where indicated, anti-Xpress monoclonal Ab (mAb) (1:50, Invitrogen, ThermoFischer Scientific, Rockford, IL, USA) was used to detect MLC1 protein by exploiting the Xpress epitope cloned at the NH_2 terminal of the recombinant proteins. As secondary Abs, a biotinylated goat anti-rabbit IgG H + L Ab (4.3 μg/ml; Jackson Immunoresearch Laboratories, West Grove, PA) followed by streptavidin-TRITC (2 μg/ml; Jackson) and Alexa Fluor 488 goat anti-mouse IgG Ab (1:300, Invitrogen, ThermoFischer Scientific) were used. Coverslips were washed, sealed in Fluoroshield with 40,6-diamidino-2-phenylindole (DAPI, Sigma-Aldrich) and analyzed with a fluorescence microscope (Carl Zeiss, Jena, Germany), equipped with a digital camera (ZEISS Axiocam 512); images were acquired by using ZEN 3.1 blu edition software. To quantify the IF and monitor changes in plasma membrane expression of the MLC1 protein, the distribution of immunofluorescence pixel intensity along a freely defined line (indicated by a dotted arrow in the IF images), spanning the whole cell (plasma membrane-cytoplasm-plasma membrane), was evaluated using the profile analysis tool of the NIH ImageJ software as previously described (Brignone et al., 2019). Colocalization of CaM and MLC1 proteins was evaluated by Pearson's correlation coefficient (PCC). Significant differences between samples were calculated using unpaired two-tailed Student *t*-test ($^*p < 0.05$, $^{**}p < 0.01$, $^{***}p < 0.001$).

2.4. Protein extraction and western blotting (WB)

Total protein extracts from astrocytoma cell lines and mouse astrocytes were obtained as previously described (Lanciotti et al., 2012). Equal amounts of proteins (30 or 40 μg) were resolved on SDS–PAGE using gradient (4–12%) pre-casted gels (Invitrogen, ThermoFisher Scientific) and transferred onto a nitrocellulose membrane using the Trans-Blot Turbo Transfer System (BioRad, Hercules, CA, USA). Nitrocellulose membranes were blotted overnight (ON) at 4 °C using anti-MLC1 pAb (1:1500), in-house generated (Ambrosini et al., 2008), anti-β-Actin mAb (1:2000, Santa Cruz Biotechnology), anti-GST mAb (1:1000, Santa Cruz Biotechnology), anti-CaM pAb (1:50, Santa Cruz Biotechnology), anti-GAPDH mAb (1:1000, Santa Cruz Biotechnology), anti-phospho-ERK1/2 (Thr202/Tyr204) mAb (1:1000, Cell Signaling Technology), anti-phospho-EGFR mAb (1:1000; Abcam, Cambridge, UK), anti-pCaMKII pAb (1:200, Santa Cruz Biotechnology) and anti-Xpress mAb (1:2000, Invitrogen, ThermoFisher Scientific). After 3 washings in Tris buffered saline (TBS), membranes were incubated with horseradish peroxidase-conjugated anti-mouse or anti-rabbit Abs (1:5000; BioRad Laboratories) for 1 h at RT. Immunoreactive bands were visualized using an enhanced chemiluminescence reagent (Thermo Scientific) and exposed on a BioRad ChemiDoc XRS system. Densitometric analyses of WB experiments were performed using NIH ImageJ software or BioRad ChemiDoc XRS system. Quantification of protein loading content was carried out using a bicinchoninic acid assay (Pierce BCA protein assay kit; Thermo Scientific).

2.5. Fura-2-based Ca^{2+} imaging

Cytoplasmic Ca^{2+} was measured by the fluorescence video-imaging technique with the Ca^{2+} indicator Fura-2-AM (Invitrogen, ThermoFisher Scientific). U251 cells seeded on PLL treated glass coverslips, were kept in the dark (50 min) with 2 μM Fura-2-AM dissolved in recording buffer (see below) at RT. Loading and recording buffer had the following composition (mM): 140 NaCl, 5 KCl, 1 $MgCl_2$, 2.5 $CaCl_2$, 5.5 D-glucose, 10 HEPES/NaOH at RT, pH 7.4). In Ca^{2+}-free solutions, Ca^{2+} was replaced by $MgCl_2$ and 0.5 mM EGTA was added (0-Ca^{2+} solution). Coverslips were placed in the perfusion chamber on the stage of an inverted microscope (Axiovert 35, Zeiss, Germany) and perfused with buffer solution. To avoid the contamination of even the least amount of Ca^{2+}, for Ca^{2+}-free experiments also the perfusion chamber was filled with 0-Ca^{2+} solution. A custom-made local solution exchange system allowed the solution bathing the cells to be rapidly switched between control and test solutions. Excitation wavelengths at 340 and 380 nm were applied every 2 s (*sec*) by a monochromator (Polychrome II, Photonics, Germany) and the emitted light (510 nm) was recorded by a CCD digital camera (PCO, Sensicam, Germany) connected to a computer. The Imaging Workbench software (INDEC Systems, CA, USA) was used for recording and initial data analysis. Origin 7.5 software (Microcal Software, USA) was used for further analysis and graphical presentation. Ca^{2+} concentrations were expressed as the ratio of emissions at 340 nm to 380 nm.

2.6. Calmodulin-binding prediction

To predict computationally CaM binding to MLC1, we used the following CaM target database: http://calcium.uhnres.utoronto.ca/ctdb/ctdb/sequence.html. Scores are normalized on a scale from 0 to 9, where 0 indicates a low and 9 a high probability of CaM binding.

2.7. Recombinant protein preparation and calmodulin binding assay

The N-terminal and C-terminal cytoplasmic regions of human MLC1 (aa 1–56 and aa 320–377) fused with GST were obtained in BL21 *Escherichia coli* and purified by affinity chromatography as previously described (Lanciotti et al., 2010). GST and GST fusion protein were used in in vitro protein binding as previously described (Lanciotti et al., 2010). Agarose–bound CaM (Sigma-Aldrich) (100 μl of 50% suspension) equilibrated in 150 mM NaCl, 20 mM Tris-HCl pH 7.4 and 2 mM $CaCl_2$ was incubated with 200 μg GST-MLC1 N-terminal (GST-MLC1-N-t), C-terminal (GST-MLC1-C-t/GST-MLC1-C-t-Mut) region ON at 4 °C. After extensive washes with equilibration buffer without $CaCl_2$, bound proteins were eluted with equilibration buffer containing 10 mM EDTA and analyzed by WB. For the generation of GST-MLC1-C-t-Mut peptide carrying mutations of the isoleucine/glutamine aa sequence (IQ) present in the MLC1 CaM binding motif into an alanine/glycine sequence (AG), oligonucleotides were generated carrying nucleotide substitution (ATC CAG was substituted with GCC GGG). Primers containing the nucleotide substitutions and the *Eco*RI/*Xho*I restriction sites at their extremities were used to amplify pGEX-MLC1-C-t plasmid (Lanciotti et al., 2010) by RT-PCR. PCR products were then cloned in pGEX plasmid (Addgene Europe, LGC Standards,Teddington, UK) at EcoRI-XhoI restriction sites. For PCR reaction the following conditions were used: sense primer 5′-ccgaattccacgggcaccgccgccgggtgcgtgcgcttcaaggtc-3′; antisense primer 5′-gggactcgagtcactgggccatttgcac-3′. PCR was executed at 94 °C x 1′ for 1 cycle and then for 35 cycles at 94 °C x 1′, 60 °C x 1′, 72 °C x 1′ with 7′ at 72 °C for the final extension reaction. PCR product obtained was run on agarose gel and extracted/purified with a Gel Extraction Kit (Qiagen, Hilden, Germany) and cloned followed the procedures described in Lanciotti et al. (2010). The plasmid DNA obtained was sequenced to confirm the presence of the in-frame mutation (Eurofins, Genomics). Plasmids containing the correct aa substitutions were transformed in BL21 *Escherichia coli* cells and used to express recombinant mutated

GST-MLC1-C-t-Mut peptide for CaM binding assay.

2.8. Histidine co-purification

Biochemical enrichment of histidine-tagged proteins was obtained as described before (Lanciotti et al., 2010; Lanciotti et al., 2012; Brignone et al., 2014). Briefly, pellets obtained from the astrocytoma cell line (about 1×10^7 cells) were re-suspended in a buffer solution containing 150 mM NaCl, 10 mM HEPES, 1 mM EGTA, 0.1 mM $MgCl_2$ pH 7.4, 0.5% Triton X-100 and a protease inhibitor cocktail (Sigma), incubated on ice for 20 min and then centrifuged at 16,000 $\times g$ for 10 min at 4 °C. The supernatants obtained, diluted to a final concentration of 10 mM imidazole, were incubated ON at 4 °C with 100 µl (50% *v*/v suspension) of Ni-NTA Agarose resin (Qiagen, Hilden, Germany) with gentle rocking. After extensive washing, protein elution was carried out using imidazole, at a concentration of 200 mM. The eluted proteins were analyzed by SDS–PAGE and WB.

2.9. Calmodulin affinity purification

Mouse brain homogenate obtained by lysis with RIPA buffer and centrifugated at 14,000 g at 4 °C for 15 min, was diluted to a final concentration of 150 mM NaCl, 20 mM Tris-HCl pH 7.4 and 2 mM $CaCl_2$ (binding buffer) and then incubated ON at 4 °C with gentle rocking for the affinity purification of calmodulin binding proteins with CaM resin (Sigma-Aldrich; 100 µl of 50% suspension), previously equilibrated in binding buffer. Following extensive washings with binding buffer without $CaCl_2$, protein elution was carried out using 150 mM NaCl, 20 mM Tris-HCL pH 7.4 and 10 mM EDTA and analyzed by WB.

2.10. Volume measurement by Calcein-quenching method

The calcein-quenching method was applied to cell cultures to record volume changes induced by hyposmotic shock. U251 astrocytoma cell lines were exposed to a 5 µM calcein containing solution for 30 min at 37 °C, and washed for 10 min before recording. Glass coverslips harboring Calcein-loaded U251 cells were placed in a recording chamber on the stage of an inverted microscope (Zeiss, Axiovert 35) and perfused with a pre-warmed (35 °C; TP2 Temperature Controller, Cell Micro Channels) saline solution of the following composition: 140 NaCl, 5 KCl, 2 $CaCl_2$, 2 $MgCl_2$, 5 HEPES 20 Glucose (mM, pH 7.4). An excitation λ of 488 nm was applied by a monochromator (Till Photonics, Polychrome II) at an interval of 10 s and the emission fluorescence was collected by a ccd camera (PCO, Sensicam). A gravity driven perfusion system allowed the change from isosmotic to hyposmotic solutions. This latter was obtained by mixing the above solution with the same volume of a solution in which NaCl was omitted (0-Na solution), to have a 40% decrease of osmolarity. The experimental protocol consisted in a 3 min recording in isosmotic solution followed by a 10 min recording in hyposmotic solution, during which a fluorescence raise depicting volume increase was followed by a fluorescence intensity decrease, depicting regulatory volume decrease (RVD). The fluorescence signal was recorded as ΔF/F0 (F = fluorescence intensity; ΔF=Ft-F0). To compare RVD from different cell lines, fluorescence intensity trace from each cell was normalized to the maximum valued and traces from the same line were averaged and shown in the time-course graph.

2.11. Statistical analysis

All the statistical analyses were performed using GraphPad prism software (USA). Results were expressed as mean ± standard deviation (SD). Data were first subjected to normality test (D'Agostino and Pearson Omnibus Normality test); when data followed a normal distribution, a Student-*t*-test was applied; otherwise, non-parametric tests, such as Wilcoxon test or Kruskal-Walli's test, followed by Dunn's Multiple Comparison post hoc test when necessary. Statistically significant *p* values are * $p < 0.05$, ** $p < 0.01$ and *** $p < 0.001$, while not significant data are indicated with the "ns" abbreviation.

3. Results

3.1. Intracellular Ca^{2+} release but not capacitive calcium entry affects MLC1 protein assembly and trafficking to the plasma membrane in human U251 cells and primary mouse astrocytes

Using U251 astrocytoma cells stably expressing the wild-type (MLC1-WT) or the mutated MLC1 protein (MLC1-S280L), we recently reported that MLC1 phosphorylation by the Ca^{2+}/Calmodulin regulated kinase II (CaMKII) potentiates VRAC current activation in response to endoplasmic reticulum (RE) Ca^{2+} release (Brignone et al., 2022), suggesting a functional relationship between MLC1 protein and Ca^{2+} signaling in astrocytes. To elucidate further the molecular effectors linking MLC1 function to Ca^{2+} signaling, we analyzed in the same U251 cells the consequences of cytoplasmic Ca^{2+} increase on the assembly of the MLC1 dimeric form and its trafficking to the plasma membrane (PM), two conditions indicating MLC1 functional activation (Brignone et al., 2011; Lanciotti et al., 2012; Brignone et al., 2022). Since in astrocytes MLC1 is activated by stimuli (hyposmotic, inflammatory) inducing intracellular calcium release from the ER compartment, and the consequent capacitative calcium entry (CCE) needed for ER refilling (Fischer et al., 1997), we optimized an experimental protocol to distinguish between ER calcium release and CCE as potential intracellular calcium source for MLC1 activation. We stimulated cells with thapsigargin (TG), the non-competitive inhibitor of the ER Ca^{2+} ATPase pumps (SERCA), in the presence or not of the CCE inhibitor lanthanum chloride ($LaCl_3$), (Pizzo et al., 2001). SERCA pump drives cytosolic free Ca^{2+} ion entrance into the ER lumen, and its inhibition causes a massive Ca^{2+} release from the ER followed by CCE. Western blot (WB) and immunofluorescence (IF) analysis of U251 cells challenged for 5 min with 100 nM TG, a treatment leading to a rapid and sustained Ca^{2+} release in astrocytoma cells (Kovacs et al., 2005), showed an increase of the MLC1 dimeric form localized at the PM when compared to unstimulated cells (Fig. 1A, C, D, F).

A similar increase was observed when U251 cells were treated with the P2Y purinergic receptors agonist ATP (100 µM for 5 min, Fig. 1B), capable of triggering InsP3-mediated Ca^{2+} release from the ER (Pizzo et al., 2001). Accordingly, IF images of ATP-treated cells showed higher levels of MLC1 at PM when compared to untreated cells (Fig. 1C, E, F), confirming the main role of ER Ca^{2+} release on MLC1 protein assembly and sorting. The same stimulations were repeated in presence of $LaCl_3$ to evaluate CCE contribution to MLC1 dimerization and trafficking. We found that CCE did not take part in these processes, since no significant differences were observed when $LaCl_3$ was added to TG/ATP-containing solutions (Fig. 1A, B).

As observed in astrocytoma cells, also in primary mouse astrocytes TG and ATP increased the endogenous MLC1 dimeric form with no effect of $LaCl_3$ addition (Fig. SD1A, B, arrows).

To exclude that increased MLC1 protein trafficking was due to unspecific protein release from ER induced by TG/ATP treatment, we also analyzed U251 cells stably expressing MLC1 carrying the pathological S280L mutation (MLC1-S280L) known to be a protein mainly localized into ER and with the dimeric form strongly reduced (Lanciotti et al., 2012; Lanciotti et al., 2016; Brignone et al., 2019). These experiments showed no changes in the mutant protein dimerization in response to the above treatments (Fig. SD2A, B), confirming that only the MLC1-WT is sensitive to intracellular Ca^{2+} changes. In the same conditions of TG and ATP stimulations, we did not observe any oligomerization of the potassium (K^+) channel Kir2.1 when stably transfected in U251 cells (Ambrosini et al., 2014), further excluding possible unspecific effects of the calcium release-inducing treatments on protein assembly processes (Fig. SD2C).

Overall, these findings disclose that MLC1 is a Ca^{2+} responsive

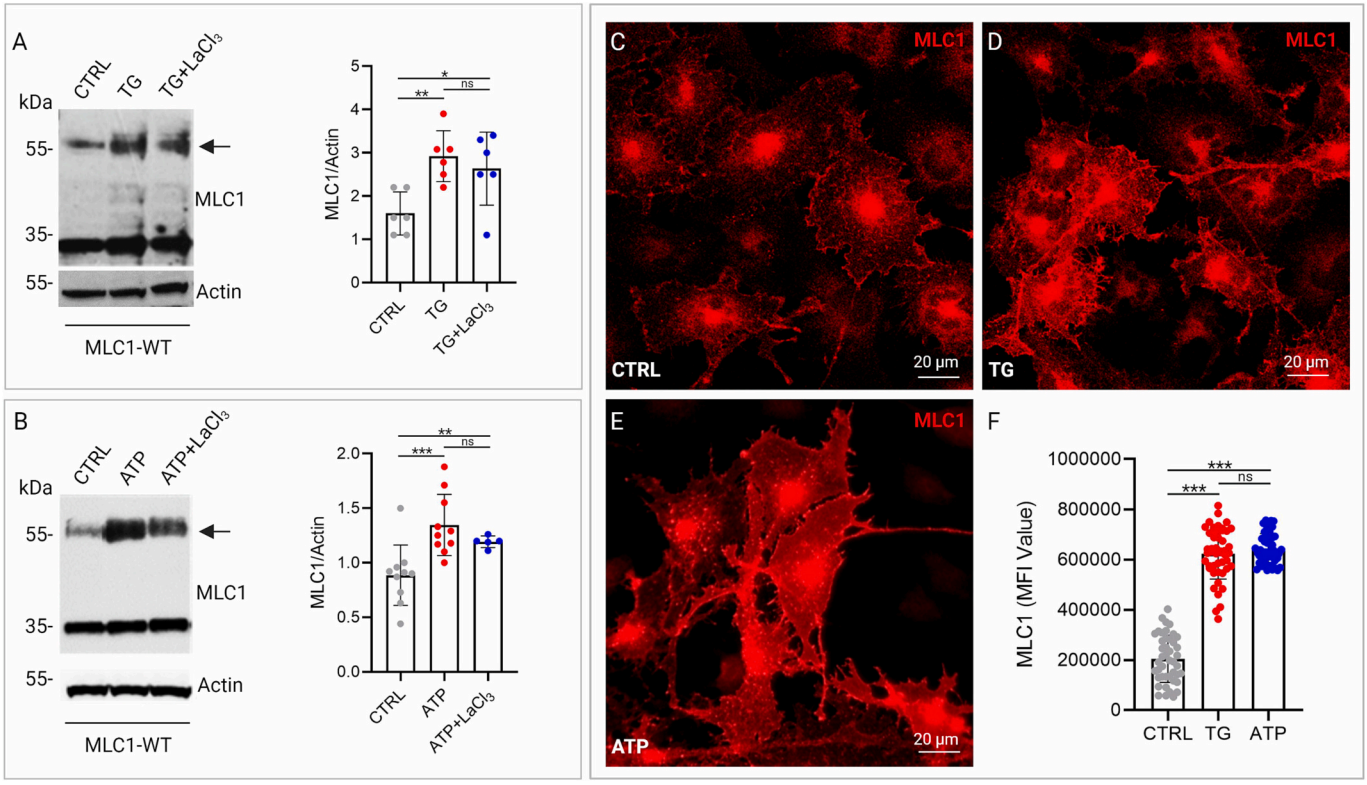

Fig. 1. Calcium release induced by thapsigargin (TG) and ATP stimulation affects MLC1 dimerization and translocation to the plasma membrane (PM) in U251 cells. (A, B) WB analysis to monitor wild-type MLC1 protein expression in U251 cell lines (MLC1-WT) shows upregulation of MLC1 dimers (arrows) after cell stimulation with TG (5 min, 100 nM) or ATP (5 min, 100 µM). MLC1 dimer expression is not affected by TG or ATP co-treatment with 100 µM of Lanthanum Chloride (TG + $LaCl_3$ and ATP + $LaCl_3$ in A, B respectively). Actin is used as a loading control. Molecular weight (MW) markers are indicated on the left (kDa). The bar graphs represent the densitometry analysis of the MLC1 protein dimer bands normalized with the amount of actin in the corresponding samples. The means ± SD of 5–10 independent experiments for each condition are shown. Statistical differences were calculated using non-parametric tests (*$p < 0.05$; **$p < 0.01$; ***$p < 0.001$). (C-E) IF staining of U251 cells expressing MLC1-WT using anti-MLC1 pAb (red) show increased expression of MLC1 at PM after cell treatment with TG (D) or ATP (E) when compared to untreated cells (CTRL, C). Scale bars: 20 µm. (F) The bar graph shows the means ± SD values of fluorescence intensity (MFI) of 3 independent experiments where 40–50 cells/condition were analyzed. Significant differences between control and treated cells expressing MLC1-WT were calculated using one-way ANOVA, unpaired two-tailed Student *t*-test (***$p < 0.001$). This figure was partially created with BioRender.com.

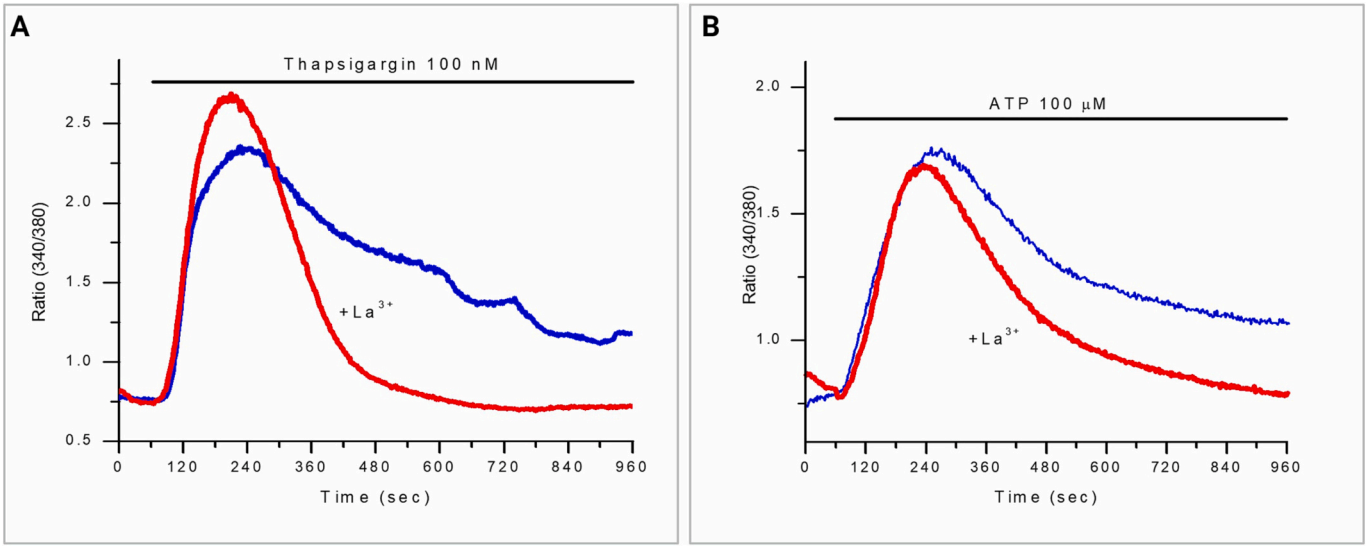

Fig. 2. Ca^{2+} movements in U251 cells in response to treatments inducing MLC1 trafficking.
To monitor the source of Ca^{2+} stimulating changes in MLC1 trafficking, TG and ATP were applied for 15 min to U251 cells expressing MLC1-WT. As depicted by the exemplifying Fura-2 Ca^{2+} recordings, TG (A) and ATP (B) induced Ca^{2+} transients due mainly to Ca^{2+} release from ER and Ca^{2+} entry from ER-depletion activated channels (capacitative Ca^{2+} entry, CCE, blue lines). The application of the same agents in the presence of Lanthanum (La^{3+}) caused Ca^{2+} transients only due to release of the ion from ER (red lines), as expected.

protein whose assembly and trafficking are favored by Ca^{2+} release from intracellular stores but not by CCE.

To confirm the intracellular Ca^{2+} sources stimulating MLC1 activation in U251 cells and validate treatment specificity, we analyzed the Ca^{2+} transients induced by the application of the same concentrations of the above-mentioned agents using Fura-2-based fluorescence video-imaging. Fifteen min application of TG and ATP to U251 cells induced a fast-raising Ca^{2+} transient followed by a slow decreasing plateau phase, which was absent when recording in the presence of $LaCl_3$ (100 μM, 15 min). Such time-course was compatible with a fast release of Ca^{2+} from the internal stores followed by CCE, which was abrogated by the trivalent cation La^{3+} (Fig. 2A, B).

3.2. Identification of a Calmodulin binding site at the COOH-terminal of the MLC1 protein

To further clarify the features conferring Ca^{2+} sensitivity to the MLC1 protein, we first analyzed the MLC1 primary aminoacidic (aa) sequence using different protein databases and found that a putative calmodulin (CaM) binding consensus motif was present at the COOH terminal domain of the MLC1 protein (aa 323–339; http://calcium.uhnres.utoronto.ca/ctdb/ctdb/home.html) (Fig. 3A). CaM is a Ca^{2+}–binding protein ubiquitously expressed in eukaryotes able to regulate in a Ca^{2+}-dependent manner biological activities of many cellular proteins, including ion channels and transporters (Swulius and Waxham, 2008; Kovalevskaya et al., 2013; Urrutia et al., 2019). At the cytoplasmic Ca^{2+} concentration [Ca^{2+}] of a quiescent cell (10^{-7}–10^{-8} mol l^{-1}), CaM has virtually no Ca^{2+} bound, and is inactive. It, however, undergoes rapid activating conformational changes as cytoplasmic [Ca^{2+}] rises upon Ca^{2+}-elevating stimuli. The Ca^{2+}-CaM complex is now capable of interacting with specific target proteins containing the CaM binding motif, like the CaMKII, which are generally unable to bind Ca^{2+} directly but use CaM as a Ca^{2+} sensor and signal transducer (Yaduvanshi et al., 2021). To verify whether MLC1 interacted with CaM through the specific COOH terminal motif, we performed a CaM binding assay using CaM-agarose resin and recombinant MLC1-NH_2 or MLC1-COOH terminal domains fused to glutation-S-transferase: GST-MLC1-NH_2 (N-terminal aa 1–56, N-t) and GST-MLC1-COOH (C-terminal aa 320–377, C-t). In

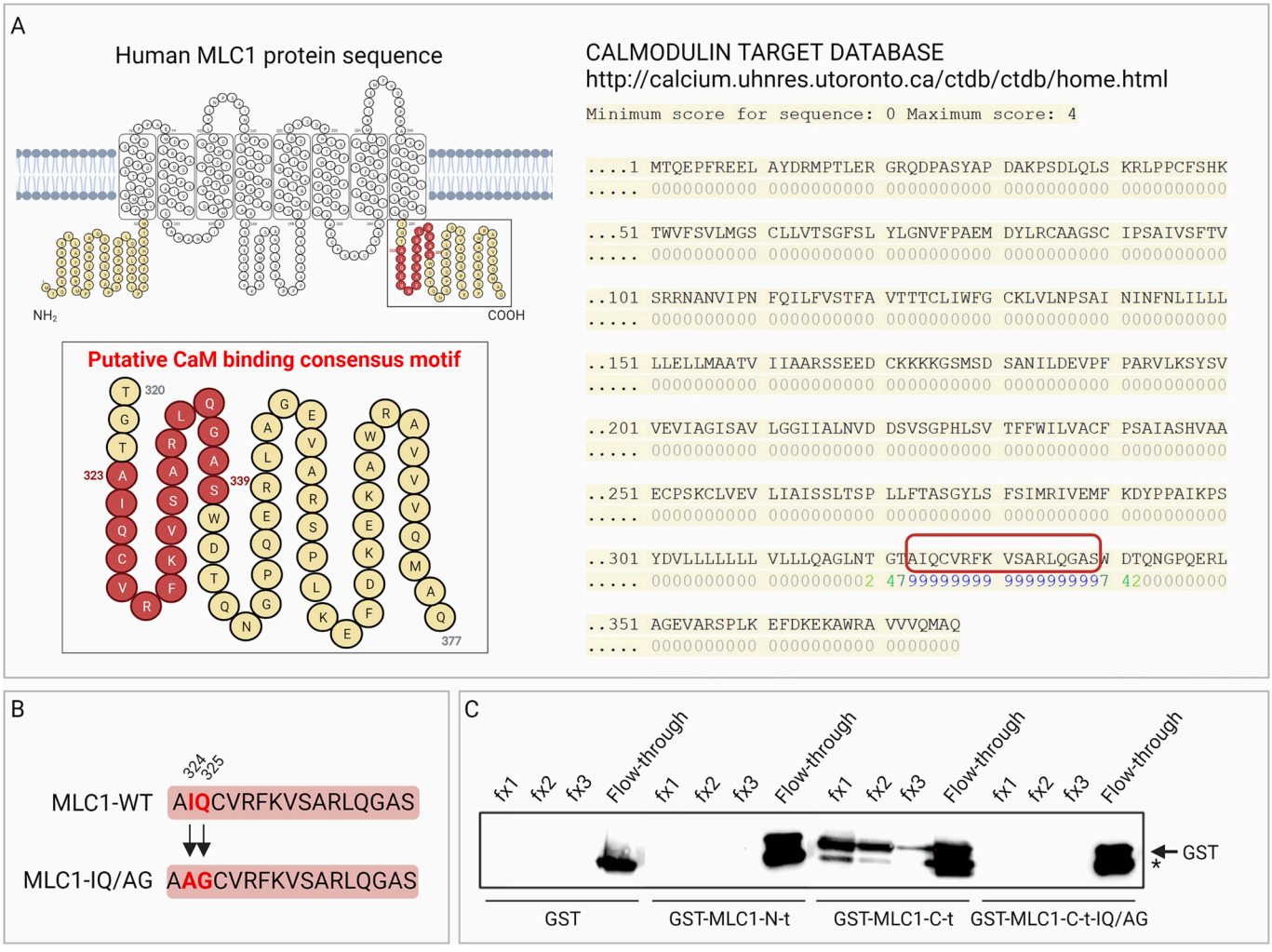

Fig. 3. Calmodulin (CaM) binds the COOH terminal of the MLC1 protein.
(A) Schematic representation of the human MLC1 protein sequence showing the NH_2 and COOH domains (yellow) and the putative CaM binding consensus motif identified at the C-terminal domain (amino acids, aa, 323–339, red) by the protein database http://calcium.uhnres.utoronto.ca/ctdb/ctdb/home.html. (B) Aa modifications performed to generate MLC1 carrying CaM-binding site mutations. The IQ aa sequence (aa 324–325) of the MLC1-WT protein was substituted with an alanine/glycine (AG) sequence (MLC1-IQ/AG). (C) Pull-down assay using CaM-agarose resin and recombinant MLC1-NH_2 (N-terminal, aa 1–56, N-t) or MLC1-COOH (C-terminal, aa 320–377, C-t) terminal domains or the mutant IQ/AG MLC1-C-t fused to glutathione-S-transferase (GST-MLC1-N-t, GST-MLC1-C-t, GST-MLC1-C-t-IQ/AG, respectively). GST peptide alone was used as negative control. WB analysis using anti-GST antibody of the eluted proteins fractions (fx) 1–3 shows that CaM/MLC1 binding occurs only with the GST-MLC1-C-t, and not with the GST-MLC1-N-t or GST-MLC1-C-t-IQ/AG. The starting material is indicated as Flow-through. Asterisk indicates a GST fusion protein degradation product recognized by the anti-GST pAb. This figure was partially created with BioRender.com.

addition, as a further control, we also performed the assay by using a GST-MLC1-COOH peptide carrying specific aa mutations in the identified CaM binding region (GST-MLC1-C-t-IQ/AG). Since isoleucine (I) and glutamine (Q) represent the invariable amino acids specifically characterizing the IQ/IQ-like CaM binding motif of CaM target proteins (O'Day and Huber, 2022), we mutagenized the IQ aa sequence into alanine (A) and glycine (G) (Fig. 3B). The binding to CaM-agarose was carried out in presence of Ca^{2+} and the bound proteins were eluted with EDTA. These experiments demonstrated that CaM/MLC1 binding occurs only when the MLC1-C-t, and not the MLC1-N-t peptide or the mutated MLC1-C-t-IQ/AG, was used (Fig. 3C), in agreement with the presence of the putative CaM consensus sequence in this domain. These findings also indicated that the IQ aa sequence at position 324–325 of the MLC1 protein is critical for MLC1/CaM interaction, as documented in other membrane proteins (Joiner et al., 2001; Etxeberria et al., 2008).

3.3. CaM interacts with MLC1 in cultured astrocytes and in mouse brain tissue

To study CaM-MLC1 interaction also in the whole cells, a co-purification assay using Histidine affinity resin was set up as previously described (Lanciotti et al., 2010; Lanciotti et al., 2012; Brignone et al., 2014) to precipitate MLC1 protein and its interactors from U251 cells by exploiting the 6-His tag present at the NH_2 terminal of the MLC1 recombinant protein. The assay was carried out in control conditions and after stimulation with ATP (100 μM, 5 min) to induce Ca^{2+} release and the consequent CaM activation, and favor MLC1 trafficking and function (Fig. 1, and Brignone et al., 2022). Fig. 4A shows that using this assay, CaM was found among the MLC1 interacting proteins in ATP stimulated cells.

We also verified whether CaM-MLC1 interaction occurred in mouse brain tissue. To this aim, we used a CaM-bound resin for the affinity purification of calmodulin-binding proteins from mouse brain tissue homogenates. With these experimental setting, the monomeric and dimeric forms of the MLC1 were detected among CaM interactors along with the CaMKII protein analyzed as positive control of the whole experimental procedure (Fig. 4B).

Altogether, these findings validate the occurrence of CaM binding to MLC1 protein in cultured astrocytes and in the brain tissue.

3.4. CaM inhibition arrests MLC1 trafficking to the PM

Once established MLC1/CaM interaction, we wanted to verify whether CaM binding was responsible for the MLC1 protein assembly and trafficking to the PM induced by ER Ca^{2+} release, as it occurs to several PM proteins, including numerous ion channels and receptors (Joiner et al., 2001; Roncarati et al., 2005; Etxeberria et al., 2008; Lee et al., 2008; Kovalevskaya et al., 2013; Roig et al., 2021). To this aim, WB and IF analyses of U251 cells in control conditions and after 5 min of ATP stimulation were performed in presence or absence of the CaM antagonist Calmidazolium (CMZ; 1 μM, Sunagawa et al., 1999). These experiments confirmed that ATP favors MLC1 dimer formation (Fig. 5A) and trafficking to the PM (Fig. 5B, C) and revealed that both processes were strongly inhibited by the co-treatment with the CaM specific inhibitor CMZ (Fig. 5A, D, K). Interestingly, IF staining of MLC1-WT expressing cells after treatment with ATP also showed an increase of MLC1-CaM co-localization in the perinuclear areas that was inhibited by CMZ treatment (Fig. 5I–L). Noteworthy, in the same cells, 15 min hyposmotic stimulation activating ER Ca^{2+} release and MLC1 assembly/trafficking (Brignone et al., 2022) favored MLC1/CaM colocalization (Fig. SD3). As expected, CMZ treatment abolished MLC1 assembly/trafficking also in response to hyposmotic stress (Fig. SD4). These data are consistent with the view that the binding of the Ca^{2+} sensor CaM to MLC1 protein favors dimer association and protein translocation to the PM, thus conferring Ca^{2+} dependence to these events.

3.5. CaM regulates MLC1 functions: generation and functional characterization of U251 cells expressing MLC1 carrying mutations in the CaM-binding site

To more directly assess the functional consequences of CaM binding to MLC1, we generated U251 cells expressing MLC1 protein carrying

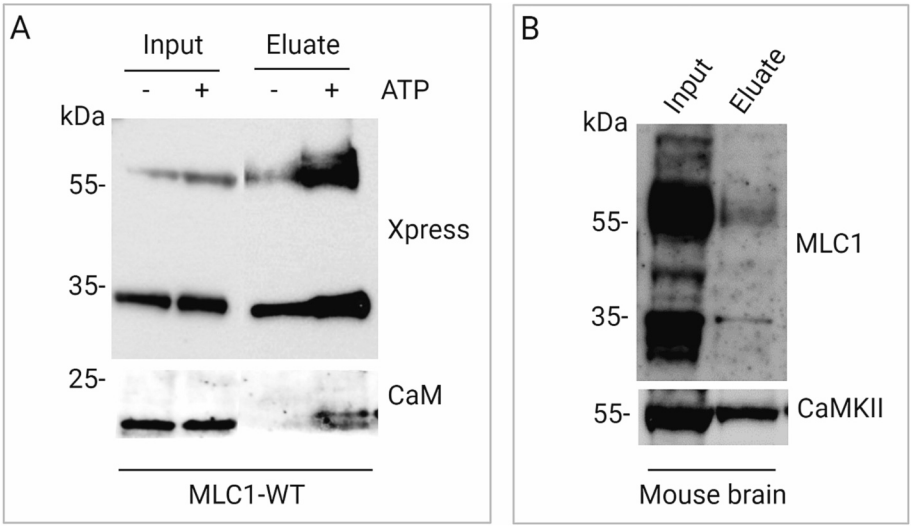

Fig. 4. CaM interacts with MLC1 in U251 astrocytoma cells and mouse brain tissue.
(A) A Histidine (His) co-purification assay to verify calmodulin (CaM) association to MLC1 was performed in U251 cells. Total fractions (Input) from U251 cells expressing MLC1-WT in control conditions (−) or after 5 min of ATP treatment (+) were co-purified using Ni-NTA agarose and eluted with 200 mM Imidazole (Eluate) to enrich and purify His-tagged MLC1 and its interactors. WB analysis on Input and Eluate proteins using an anti-Xpress mAb (recognizing the X-press epitope in the MLC1 protein sequence) and a CaM pAb, shows that CaM interacts with MLC1-WT cells after ATP stimulation. One representative experiment out of three is shown. MW markers are indicated on the left (kDa). (B) A pull-down assay was performed using CaM-agarose resin and mouse brain extract. WB analysis of protein eluates (Eluate) reveals the binding of MLC1 protein to CaM. CaMKII was used as a positive control. The starting material derived from mouse brain extract is indicated as Input. MW markers are shown on the left (kDa). One representative experiment out of 3 performed is shown. This figure was partially created with BioRender.com.

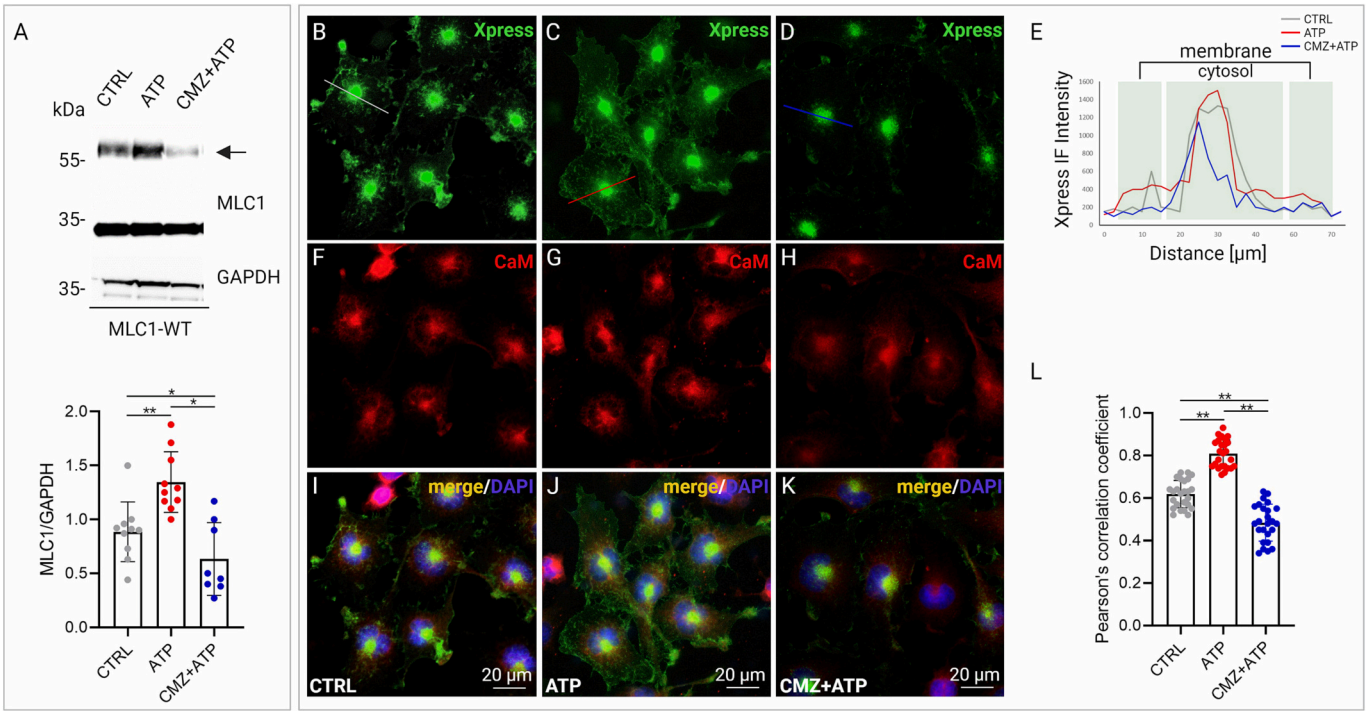

Fig. 5. CaM inhibition by Calmidazolium affects MLC1 dimerization and protein trafficking to the PM in response to ATP stimulation in U251 cells.
(A) WB analysis of U251 cell expressing MLC1-WT shows a significant increase of the dimeric, PM-associated form of MLC1 (arrow) following a 5 min treatment with ATP and a reduction after cell co-treatment with calmidazolium (CMZ + ATP) when compared to untreated cells (CTRL). GAPDH is used as a loading control. MW markers are indicated on the left (kDa). The bar graph below the WB represents the densitometry analysis of the MLC1 dimericbands (arrow) normalized with the amount of GAPDH in the corresponding samples. The means ± SD of 8–10 independent experiments are shown. Statistical differences were calculated using non-parametric tests (*$p < 0.05$; **$p < 0.01$). (B—K) IF staining of U251 MLC1-WT cells is performed by using anti-Xpress mAb (green) in combination with anti-CaM pAb (red). Panel C and D show an increase of MLC1 expression after ATP stimulation (C), and a lower localization of MLC1 at PM following cell co-treatment with CMZ + ATP (D), when compared to unstimulated conditions (CTRL, B). (E) Distribution of Xpress IF pixel intensity along a freely defined line (representatively indicated in each IF image, panels B—D) spanning the whole cell, confirms a general and PM increase of the anti-Xpress fluorescence intensity in ATP-stimulated cells (red line) and lower fluorescence intensity peaks in CMZ + ATP co-treated cells (blue line), when compared to untreated cells (grey line). One representative intensity plot is shown for each IF panel. (F—H) IF staining for anti-CaM shows no significant variation of calmodulin protein localization between untreated and treated cells. (I—K) Double IF staining reveals an increase of MLC1-CaM colocalization in the perinuclear areas following ATP stimulation (yellow signal in J), when compared to untreated cells (I). The colocalization is inhibited by CMZ+ATP co-treatment (K). Scale bars: 20μm. Panel (L) shows the quantification of the colocalization signal (yellow) evaluated using ImageJ software. The degree of colocalization was estimated using the Pearson's correlation coefficient. Data are shown as means ± SD of 25 cells for each condition (** $p < 0.01$, unpaired two-tailed Student's t-test). This figure was partially created with BioRender.com.

mutations in the CaM binding site. Following the results reported above indicating the importance of the IQ aa sequence in this interaction, the same modifications of the COOH terminal sequence (IQ/AG) used for the pull-down assay (Fig. 3B, C) were reproduced in the construct used to generate the mutant cell lines, as described in the MM section. The morpho-functional characterization of cells stably expressing MLC1 with CaM binding site mutations (MLC1-IQ/AG) by WB and IF revealed that changing of the specific CaM signature strongly affected MLC1 distribution and dimerization. Indeed, the MLC1-IQ/AG protein was found mainly confined into perinuclear ER compartment of the U251 cells, and MLC1 dimerization strongly decreased similarly to what reported for the MLC1-S280L mutant protein (Fig. 6A, B). The same WB experiments also showed that the MLC1-IQ/AG mutations impaired the capacity of the MLC1 protein to inhibit EGFR and ERK, two signaling molecules previously found to be constitutively activated in U251 cells and downregulated in WT, but not in mutant MLC1 expressing cells (Fig. 6B), (Lanciotti et al., 2016; Brignone et al., 2019).

To demonstrate that CaM binding site mutations are effective in blocking CaM/MLC1 interaction, we repeated a co-purification assay using Histidine affinity resin (His column), as reported above (Fig. 4A), to precipitate the His-tagged MLC1 protein and its interactors from U251 cells expressing MLC1-WT or the mutant MLC1-IQ/AG. Fig. 7 shows that CaM was eluted from the His column containing protein extract of MLC1-WT cells stimulated with ATP, but not of all the other cell samples. These data confirmed that IQ/AG mutations block CaM binding to the MLC1 protein and that this binding occurs only when CaM is activated by the increase of cytoplasmic Ca^{2+} levels, here obtained by ATP stimulation.

To provide a conclusive proof of the functional significance of CaM/MLC1 interaction, we then monitored whether the MLC1-IQ/AG changes affected the MLC1-mediated activation of RVD in response to hyposmotic stimulation previously observed in U251 cells (Brignone et al., 2022). The results shown in Fig. 8 indicate that hyposmotic stress induced an increase of cell volume with similar kinetic in all lines tested (i.e. MLC1-WT, MLC1-S280L, MLC1-IQ/AG). Conversely, regulatory volume decrease (RVD), depicted by the slowly decline of the fluorescence signal following volume increase, was significantly faster in WT cells compared to both MLC1-S280L and MLC1-IQ/AG cells, in keeping with a positive regulation of MLC1-WT on RVD and of the role played by CaM-MLC1 in such effect.

4. Discussion

Mutations in the astrocyte specific protein MLC1 cause progressive myelin vacuolation, and increased water content in MLC brain. Thus, the identification of MLC1 function and the molecular defects underlining this rare LD, may strongly increase our knowledge on how astrocyte control brain ion/fluid homeostasis and myelin formation and

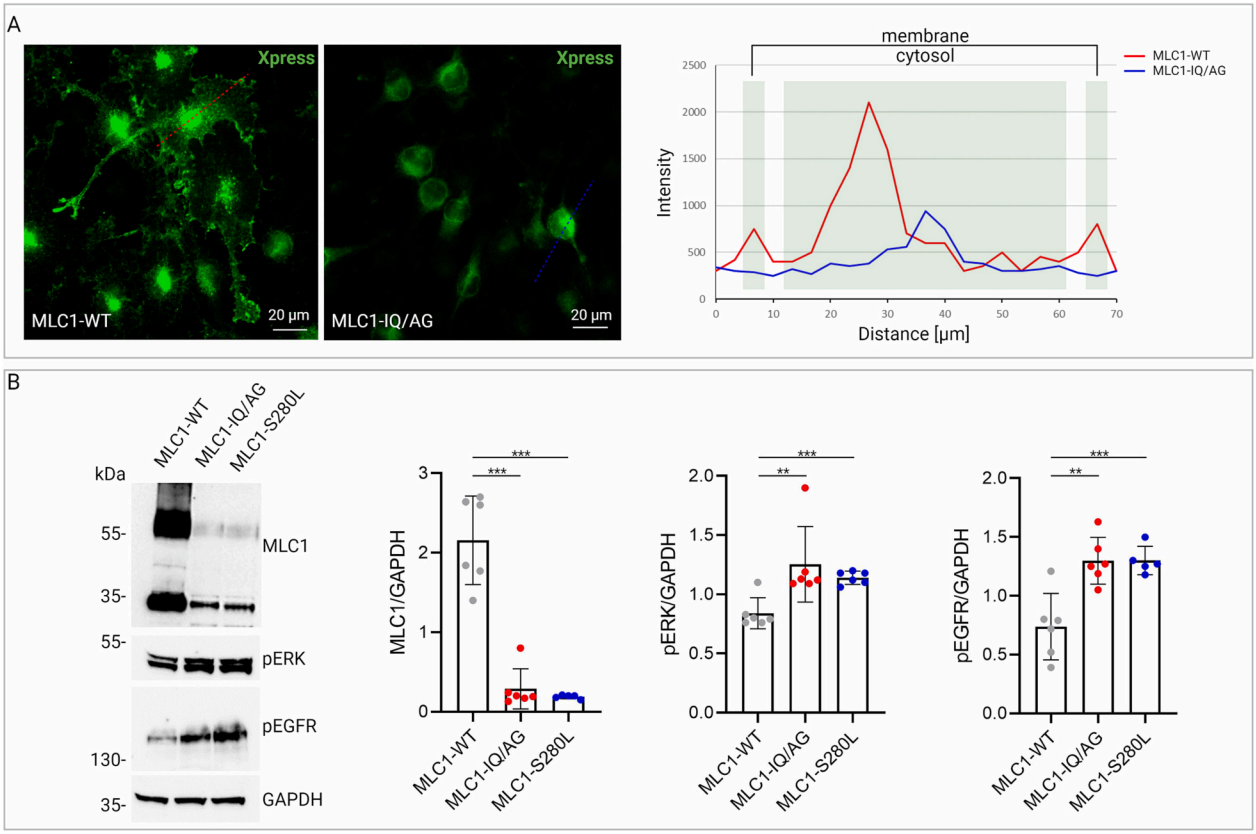

Fig. 6. Effects of CaM binding-site mutations on MLC1 assembly, trafficking and EGFR/ERK signaling pathway activation.
(A) IF staining of U251 cells expressing MLC1 wild type (MLC1-WT) and IQ/AG mutation (MLC1-IQ/AG) performed by using anti-Xpress mAb (green) shows that the MLC1-IQ/AG protein is mainly localized into perinuclear ER compartment of the U251 cells and not detectable at the PM, when compared to WT cells. The distribution of anti-Xpress IF pixel intensity along a freely defined line (representatively indicated in each IF image) spanning the whole cell, shows a very low Xpress protein fluorescence signal in PM compartment of MLC1-IQ/AG cells (blue line) when compared to MLC1-WT cells (red line). A lower Xpress protein fluorescence intensity is also observed in the cytosol of mutant versus wild type cells. One representative intensity plot is shown for each IF panel. Scale bars 20 µm. (B) WB analysis of protein extracts derived from MLC1-WT, the IQ/AG (MLC1-IQ/AG) or S280L (MLC1-S280L) mutant cells reveals an increase of ERK and EGFR phosphorylation in MLC1 mutant expressing cells when compared to MLC1-WT astrocytoma cells. GAPDH is used as a loading control. MW markers are indicated on the left (kDa). Densitometric analysis of MLC1 and phosphorylated ERK and EGFR protein bands normalized with the amount of GAPDH in the corresponding samples are shown on the right. The means ± SD of 5–6 independent experiments are shown. Statistical differences were calculated using non-parametric tests (**$p < 0.01$, ***$p < 0.001$). This figure was partially created with BioRender.com.

maintenance, paving the way towards the identification of possible pharmacological therapies for this incurable disease. To this aim, in this study we proceeded in our attempt to explore in detail the relationships and the molecular determinants linking MLC1 to Ca^{2+} signaling in astrocytes and the effects of MLC1 mutations on this axis. MLC1/Ca^{2+} signaling reciprocal regulation was previously suggested by experimental evidence demonstrating that calcium dynamics are influenced by the lack of functional MLC1 (Lanciotti et al., 2012, 2016; Petrini et al., 2013) and that MLC1 function is regulated by Ca^{2+}-induced Ca^{2+}-release (CICR) in astrocytes (Brignone et al., 2022). In addition, we also reported that in astrocytes MLC1 localizes in caveolar lipid rafts (Ambrosini et al., 2008; Lanciotti et al., 2010; Brignone et al., 2015), the PM microdomains that, by clustering Ca^{2+} channels, receptors, transporters and their regulators, operate as Ca^{2+} signal transduction platforms to modulate Ca^{2+} mediated cellular functions (Weerth et al., 2007; Pani and Singh, 2009). Interestingly, almost all the MLC1 molecular/functional interactors identified so far are transmembrane proteins structurally or/and functionally linked to caveolar lipid raft compartments. Among these, we recall GlialCAM, ClC-2, TRPV4, Na, K-ATPase, AQP4, KiR4.1, Dystrophin/dystroglycan protein complex (DGC), VRAC (Ambrosini et al., 2008; Moh et al., 2009; Noël et al., 2009; Sharma et al., 2010; Lanciotti et al., 2010; Nighot and Blikslager, 2012; Dai et al., 2013; Rezola et al., 2021; Zhu et al., 2022), along with EGFR/ERK-mediated signaling pathway components (Balbis and Posner, 2010). In addition, we recently reported that MLC1 is a CaMKII target protein, whose phosphorylation, occurring in response to CICR, stabilizes MLC1 at the PM, by reducing its degradation, and potentiates VRAC channel activity (Brignone et al., 2022). Overall, these findings converge on the idea of intracellular Ca^{2+} regulation of MLC1 functions, prompting us to elucidate further these mechanisms, also in view of the fundamental role played by Ca^{2+} signaling in astrocyte physiopathology (Verkhratsky, 2006; Shigetomi et al., 2019). MLC1 is a membrane protein subjected to rapid trafficking/recycling events (Lanciotti et al., 2010, 2012; Brignone et al., 2014, 2022). Indeed, in cultured astrocytes in basal conditions, most of MLC1 is localized at ER and perinuclear endosomal compartments (early and recycling endosomes), and it mobilizes to the PM in response to stimuli, such as ion imbalance or inflammatory stress signals (Lanciotti et al., 2012, 2016; Brignone et al., 2014, 2019) that functionally activate MLC1. All these stimulations account for rapid intracellular Ca^{2+} changes in astrocytes (Shigetomi et al., 2019; Koizumi et al., 2021), leading to suppose a direct influence of intracellular Ca^{2+} levels on MLC1 activities. To further clarify this mechanism, we here used U251 astrocytoma cell lines overexpressing WT or mutant MLC1, a cellular model in which MLC1 protein function/localization has already been extensively characterized. Using these cells, we clarified that MLC1 accumulation at the PM and acquisition of the oligomeric/active form are promoted by ER Ca^{2+} release, but not by CCE, either in response to ATP-induced stimulation of IP3R, or by means

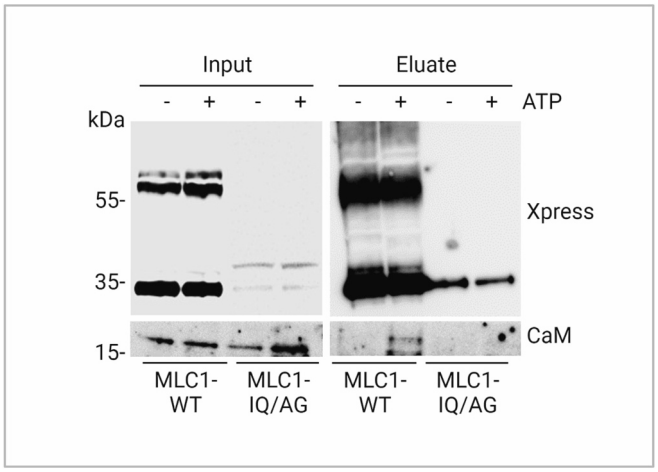

Fig. 7. CaM binding site mutations hamper MLC1-CaM interaction.
Histidine (His) co-purification assay to verify CaM association to WT or mutated MLC1 in astrocytoma cells. Total fractions (Input) from U251 cells expressing MLC1-WT or the IQ/AG mutant (MLC1-IQ/AG) in control conditions (−) or after 5 min of ATP treatment (+) were co-purified using Ni-NTA agarose and eluted with 200 mM Imidazole (Eluate), to enrich and purify His-tagged MLC1 and its interactors. Immunoblotting analysis using anti-Xpress mAb and CaM pAb shows the MLC1-CaM interaction only in U251 MLC1-WT cells after ATP stimulation. No bands related to CaM protein was observed in the eluates derived from U251 cells expressing MLC1 carrying the IQ/AG mutations. MW are indicated on the left (kDa). This figure was partially created with BioRender.com.

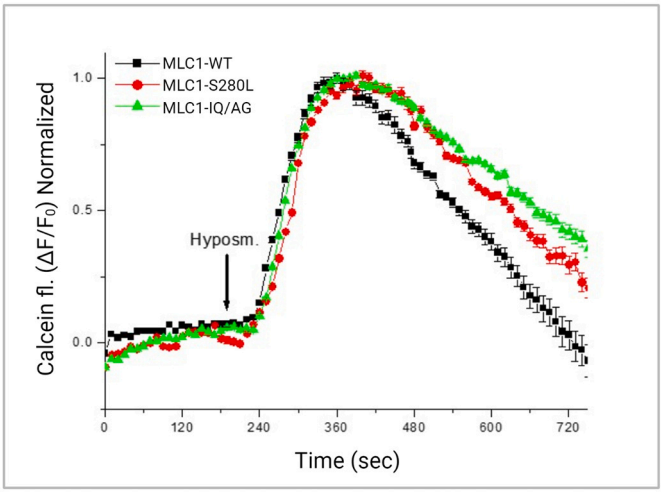

Fig. 8. Effects of CaM binding-site mutation on MLC1-induced regulatory volume decrease in U251 cells.
To monitor the change in cell volume, a hyposmotic solution was applied for 10 min to calcein-loaded cells expressing MLC1-WT, MLC1-S280L and MLC1-IQ/AG. Traces are mean ± SEM of fluorescence intensity of calcein and are normalized to their maximum value (n = 101–200 cells). Linear regression lines, calculated within the RVD phase, and depicting the speed of RVD, are superimposed to each trace. The slower RVD in MLC1-S280L and MLC1-IQ/AG cells compared to MLC1-WT cells is due to a positive modulation of RVD played by MLC1-WT and lacking in MLC1-S280L and MLC1-IQ/AG lines.

of SERCA pump inhibition, or following hyposmotic stress. In astrocytes ER Ca^{2+} release via IP3R activation is a major component of astrocytic Ca^{2+} signaling. It occurs spontaneously or is evoked by the activation of various GPCRs or receptor tyrosine kinases, and it governs several vital cellular processes like exocytosis/endocytosis, cytoskeleton polymerization, vesicular trafficking, neurotransmitter and ion uptake/release. Enhanced Ca^{2+} signals, including ER Ca^{2+} release, are frequently described in hypertrophic, reactive astrocytes (Shigetomi et al., 2019), with both beneficial or detrimental roles in various diseases or pathological conditions (Okubo, 2020 and references therein; Lim et al., 2021; Arjun McKinney et al., 2022). We here revealed that the Ca^{2+} mediated regulation of MLC1 protein trafficking and assembly occurs through the binding of CaM to its COOH terminal, being both processes inhibited by cell treatment with the specific CaM antagonist CMZ and by mutations of the MLC1-CaM binding site. It is known that in astrocytes the function of many PM proteins, particularly ion channels and transporters, including the water channels AQP4, the Ca^{2+} channel TRPV4, the Kv1.3 and SK4 potassium channels, the mGluR5 receptors, is dynamically regulated by their oligomerization, translocation and stabilization at PM favored by their interaction with CaM in response to intracellular Ca^{2+} increase (Roncarati et al., 2005; Etxeberria et al., 2008; Lee et al., 2008; Joiner et al., 2001; Kovalevskaya et al., 2013; Roig et al., 2021). MLC1 protein appeared to be similarly regulated, as demonstrated by the experiments described above. From a mechanistic point of view, it is likely that CaM binding to the MLC1 COOH terminal masks some ER retention signals, allowing the protein to exit from ER and be included in trafficking vesicles driven to the PM in response to cytoplasmic Ca^{2+} increase, as previously observed (Roig et al., 2021). The control of MLC1 trafficking by Ca^{2+} release and CaM activation in response to ATP/hyposmotic/ER stress stimulation is new evidence with important implications for the comprehension of MLC1 function in physiological and pathological conditions inducing astrocyte activation and swelling. Being localized at the interface between the brain and liquid spaces and equipped with ion channels/transporters among which AQP4/TRPV4/VRAC/Kir4.1, astrocytes are the first cells to be exposed to osmotic changes and the first cells to change their volume in response to osmotic stress or other stimulations. Noteworthy, in different in vitro and in vivo models, osmotic stress has been found to elicit robust Ca^{2+} responses at astrocyte the end-feet (Eilert-Olsen et al., 2019), a cellular domain displaying intense local Ca^{2+} activity (Denizot et al., 2019) and where MLC1 is abundantly expressed. It is conceivable that water influx through AQP4 and the consequent membrane stretch drive calcium influx via TRPV4, as previously demonstrated (Benfenati et al., 2011). We suggest that this initial Ca^{2+} influx in response to cell swelling is the trigger for ER Ca^{2+} release (CICR) then responsible for CaM/CAMKII mediated activation of MLC1 (present results and Brignone et al., 2022). Once activated and translocated at the PM, MLC1 would exert its function by potentiating further TRPV4 and VRAC channels to facilitate the release of ions/water in the perivascular space, thus decreasing astrocyte swelling and activation. Lack of MLC1 function at astrocyte end-feet may lead to their abnormal and prolongated swelling due to defective ion release (K^+, Cl^-, Ca^{2+}) with possible consequence on vascular cell properties and brain water exchanges, as observed in MLC1 KO mice (Gilbert et al., 2021) and other pathologies characterized by brain edema (Stokum et al., 2023).

Our new data revealed that being responsive to ER Ca^{2+} release, MLC1 is also responsive to other stimulations inducing IP3R activation (inflammatory mediators, purinergic receptor stimulation, ER stress signals), thus explaining previous observations of MLC1 activation in astrocyte in vitro in response to inflammatory mediators and in brain tissue affected by neuroinflammatory diseases (Lanciotti et al., 2016; Brignone et al., 2019; Brignone et al., 2022). Indeed, astrocyte activation and astrogliosis occurring in pathological conditions induce a cascade of events including intracellular Ca^{2+} and autocrine ATP release (Shigetomi et al., 2019; Okubo, 2020; Koizumi et al., 2021) that are potentially able to functionally stimulate MLC1. Once activated, MLC1 would rescue astrocyte homeostasis by turning down cell swelling and inflammatory/stress signaling pathway mediators. In other words, the capability of MLC1 to react to osmotic stress by triggering an ensemble of effectors (TRPV4, VRAC, others) deputed to regain osmotic balance might be part of a general property of MLC1 to behave as a regulator of the changes in the functional state in astrocytes. In this framework we like to recall the capability of WT MLC1 (and not mutated forms of

MLC1) to inhibit EGFR/ERK activation, pro-inflammatory potential of NF-kB/STAT3, and also the function of the astrogliosis-activated KCa3.1 potassium channel selectively expressed at perivascular astrocytes (Lanciotti et al., 2016). All this evidence leads to suppose that MLC1 overall function is to oppose to the worsening of possibly harmful conditions such as ion imbalance, volume changes, inflammatory activation, hyper-proliferation not only in oncological conditions as previously observed (Leventoux et al., 2020). To date, the exact molecular mechanism underlining the capacity of controlling such a complex ensemble of different functions is still elusive, but it is conceivable a cooperation of MLC1 with some of its known molecular interactors. According to what observed so far, the MLC1-mediated effects on its interactors could be due to changes of their phosphorylation status, directly or indirectly linked to MLC-mediated EGFR/ERK pathway regulation, as already demonstrated for VRAC and Cx43 (Elorza-Vidal et al., 2018; Lanciotti et al., 2020). In this scenario it is likely that EGFR inhibition (Lanciotti et al., 2016) is the upstream event leading to turning down this signaling cascade linked to astrocyte reactivity, but the knowledge of the MLC1-mediated molecular mechanisms causing EGFR inhibition is still incomplete. A possible explanation is that MLC1 expression favors the internalization and degradation of this receptor by modulating endocytic vesicle pH, as suggested by our previous experiments (Brignone et al., 2014; Lanciotti et al., 2016). Another candidate player in the regulatory mechanism governed by MLC1 is the non-pumping fraction of the MLC1 interactor Na, K-ATPase. Notably, the presence of the non-pumping fraction of the Na,K-ATPase in caveolar rafts regulates ERK function (Liang et al., 2007) and is involved in EGFR activation in response to astrocytes swelling (Dai et al., 2013). Interestingly, excessive activation of EGFR signaling cascade due to abnormal control of the Na, K-ATPase/EGFR axis has been observed in Batten disease, a rare inherited lysosomal storage disorder affecting the nervous system, caused by mutations in *CLN3* gene (Shematorova et al., 2018), and where abnormal calcium signaling in astrocytes has been observed (Bosch and Kielian, 2019). Astrocyte "de-activation" could be also favored by the activity of the junctional protein Cx43, whose assembly into the Gap junctions in response to hyposmosis is favored by MLC1 expression (Lanciotti et al., 2020). The MLC1-mediated increase of functional Gap junctions at astrocyte PM would allow to accelerate Ca^{2+}, ATP, K^+ and other ion dissipation in the astrocyte syncytium (Fujii et al., 2017).

The main events of these molecular mechanisms are summarized in Fig. 9.

5. Concluding remarks

The results here presented revealed that MLC is a Ca^{2+} responsive protein activated by ER Ca^{2+}-release that links extracellular stimulation and Ca^{2+} dynamics to volume regulation in astrocytes. Although more focused studies are needed to fully understand the potential bidirectional relationship between MLC1 and Ca^{2+} signaling, a very intriguing

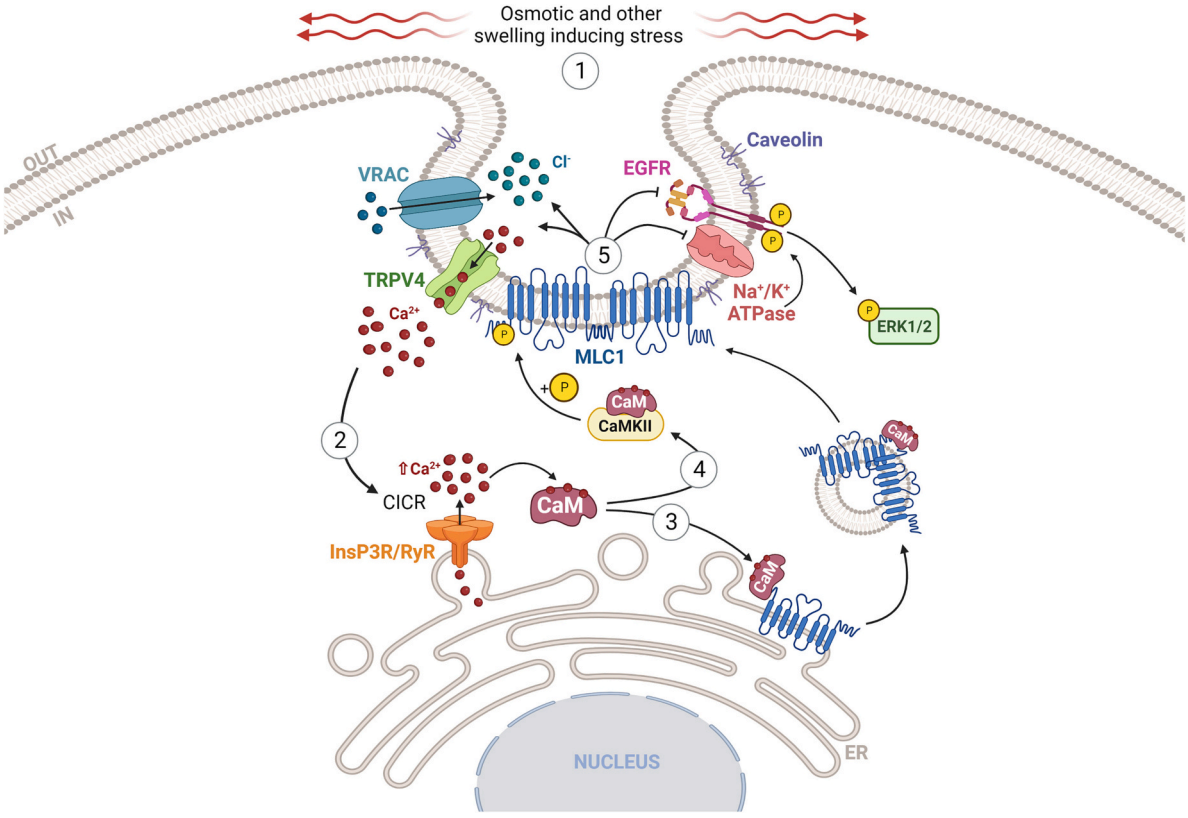

Fig. 9. Proposed molecular mechanisms of the Ca^{2+}/CaM-mediated regulation of MLC1 functions.
We integrated our view of the possible events taking place in astrocytes in response to stress signals leading to cell swelling and activation (Brignone et al., 2022) by adding Ca^{2+} release and Ca^{2+}-CaM binding as a new fundamental player of MLC1 functional activation, as follows: 1) Exposure to a hypotonic or other stimuli inducing astrocyte activation and swelling (stress signals, ionic imbalance) favors membrane stretch which induces the opening of TRPV4 and other Ca^{2+} channels; 2) Ca^{2+} release from intracellular stores through a mechanism involving Ca^{2+}-induced-Ca^{2+}-release (CIRC) mechanism; 3) Activation and binding to MLC1 COOH terminal of Ca^{2+}-CaM complex and CaM induced MLC1 assembly and trafficking to the PM; 4) MLC1 stabilization at the PM through the CaMKII-mediated phosphorylation at the NH_2 terminal (Brignone et al., 2022); 5) PM associated MLC1 is capable to potentiate VRAC (Brignone et al., 2022) and TRPV4 (Lanciotti et al., 2012) function and the consequent RVD aimed at recovering astrocyte physiological volume. Activated MLC1 is also capable to inhibit EGFR/ERK signaling, in a Ca^{2+}-CaM-dependent manner, as depicted by comparing the effect of WT-MLC1 and MLC1-IQ/AG. A possible involvement of the non-pumping caveolar Na, K-ATPase is hypothesized. This figure was created with BioRender.com.

hypothesis concerning MLC1 capability to behave as a general regulator of astrocyte functional state would see it as able of regulating Ca^{2+} signaling, as suggested by our previous results (Lanciotti et al., 2012, 2016; Petrini et al., 2013). Ca^{2+} dynamics represent a key mechanism making astrocytes capable to react to and integrate external stimulations for modulating critical functions like neuronal activity, neurovascular unit function and myelin formation and maintenance (Okubo, 2020; Zamora et al., 2020). Abnormal Ca^{2+} signaling in astrocytes is not only a consequence of pathological processes but constitutes an underlying cause common to multiple neuroinflammatory/neurodegenerative (Verkhratsky, 2006; Shigetomi et al., 2019; Koizumi et al., 2021) and also neurodevelopmental diseases (Arjun McKinney et al., 2022). Remarkably, an abnormal increase in ER Ca^{2+} release has been observed in an animal model of Alexander disease (AxD), (Saito et al., 2018), another rare LD caused by genetic mutations in the astrocytic protein GFAP. AxD shares some pathological features with MLC and represents the only other disease where myelin degeneration is due to mutations in an astrocyte-specific protein. The involvement of astrocyte IP3R-dependent Ca^{2+} release in a wide variety of brain disorders, suggested this astrocytic calcium signaling as a novel and promising therapeutic target in the CNS (Okubo, 2020). For this reason, a better knowledge of the link between MLC1 function and Ca^{2+} homeostasis can give us important clues to clarify MLC mechanisms and fuel translational studies aimed at developing possible therapies for this disease. These benefits may be exploited also for other neurological conditions where astrocyte swelling, and brain edema have a central role in the pathological process.

Declarations

Animals CD1 Swiss mice were purchased from Harlan Laboratories (San Pietro Al Natisone, Udine, Italy). The study was approved by the National Center for Animal Research and Welfare of the Istituto Superiore di Sanità and by the Italian Ministry of Health (Authorization 271/SSA/2010).

Funding

This work was supported by funds from the Italian Ministry of Health, Ricerca Finalizzata, (Grant N. GR-2013-02355882 and GR-2021-12373946 to A.L.); 5x1000 project of the Istituto Superiore di Sanità (Project code: ISS5x1000_21-949432e8c9be to A.L.) and the European Union – NextGeneration EU through the Italian Ministry of University and Research under PNRR - M4C2-I1.3 Project PE_00000019 "HEAL ITALIA" to E.A. (CUP I83C22001830006). The views and opinions expressed are those of the authors only and do not necessarily reflect those of the European Union or the European Commission. Neither the European Union nor the European Commission can be held responsible for them.

Contributions

Study conception and design: M.S.·B, A.L., T.C.P., S·V., E.A. Data curation: M.S.·B, A.L., S·V., C.D·N, E.A. Acquisition of data: M.S.·B., P. M., A.L., C. D.N., S.V, C.M., E.S.C. Investigation: M.S.B, A.L., S.V., P.M., C.M., E.S.C., E.A. Supervision: T.C.P., S.V, E.A. Writing—original draft: S.V. and E.A. Writing—review and editing: M.S.B., A.L., S.V. and E.A. All authors helped with critical reading of the manuscript and contributed to the ideas presented therein. All authors have read and approved the final version of the manuscript.

CRediT authorship contribution statement

M.S. Brignone: Conceptualization, Data curation, Investigation, Writing – review & editing. **A. Lanciotti:** Conceptualization, Data curation, Funding acquisition, Investigation, Writing – review & editing. **P. Molinari:** Data curation, Investigation. **C. Mallozzi:** Data curation, Investigation. **C. De Nuccio:** Conceptualization, Data curation. **E.S. Caprini:** Data curation, Investigation. **T.C. Petrucci:** Conceptualization, Supervision. **S. Visentin:** Conceptualization, Data curation, Investigation, Supervision, Writing – review & editing. **E. Ambrosini:** Conceptualization, Investigation, Supervision, Writing – review & editing.

Declaration of Competing Interest

The authors declare no conflict of interest.

Data availability

Data will be made available on request.

Acknowledgments

We thank Dr. Cristina Agresti and Dr. Alessia Formato for the preparation of mouse brain tissue samples and astrocyte cultures, Dr. Gianfranco Macchia for the setting up of the pull-down assays and Mrs Mimma Tripaldi for secretarial and administrative work.

Appendix A. Supplementary data

Supplementary data to this article can be found online at https://doi.org/10.1016/j.nbd.2023.106388.

References

Ambrosini, E., Columba-Cabezas, S., Serafini, B., Muscella, A., Aloisi, F., 2003. Astrocytes are the major intracerebral source of macrophage inflammatory protein-3alpha/CCL20 in relapsing experimental autoimmune encephalomyelitis and in vitro. Glia 41, 290–300. https://doi.org/10.1002/glia.10193.

Ambrosini, E., Serafini, B., Lanciotti, A., Tosini, F., Scialpi, F., Psaila, R., Raggi, C., Di Girolamo, F., Petrucci, T.C., Aloisi, F., 2008. Biochemical characterization of MLC1 protein in astrocytes and its association with the dystrophin–glycoprotein complex. Molecular and Cellular Neuroscience 37, 480–493. https://doi.org/10.1016/j.mcn.2007.11.003.

Ambrosini, E., Sicca, F., Brignone, M.S., D'Adamo, M.C., Napolitano, C., Servettini, I., Moro, F., Ruan, Y., Guglielmi, L., Pieroni, S., Servillo, G., Lanciotti, A., Valvo, G., Catacuzzeno, L., Franciolini, F., Molinari, P., Marchese, M., Grottesi, A., Guerrini, R., Santorelli, F.M., Priori, S., Pessia, M., 2014. Genetically induced dysfunctions of Kir2.1 channels: implications for short QT3 syndrome and autism-epilepsy phenotype. Hum. Mol. Genet. 23, 4875–4886. https://doi.org/10.1093/hmg/ddu201.

Arjun McKinney, A., Petrova, R., Panagiotakos, G., 2022. Calcium and activity-dependent signaling in the developing cerebral cortex. Development 149. https://doi.org/10.1242/dev.198853 dev198853.

Balbis, A., Posner, B.I., 2010. Compartmentalization of EGFR in cellular membranes: role of membrane rafts. J. Cell. Biochem. https://doi.org/10.1002/jcb.22505.

Benfenati, V., Caprini, M., Dovizio, M., Mylonakou, M.N., Ferroni, S., Ottersen, O.P., Amiry-Moghaddam, M., 2011. An aquaporin-4/transient receptor potential vanilloid 4 (AQP4/TRPV4) complex is essential for cell-volume control in astrocytes. Proc. Natl. Acad. Sci. U. S. A. 108, 2563–2568. https://doi.org/10.1073/pnas.1012867108.

Boor, P.K., de Groot, K., Waisfisz, Q., Kamphorst, W., Oudejans, C.B., Powers, J.M., Pronk, J.C., Scheper, G.C., van der Knaap, M.S., 2005. MLC1: a novel protein in distal astroglial processes. J. Neuropathol. Exp. Neurol. 64, 412–419. https://doi.org/10.1093/jnen/64.5.412.

Bosch, A., Estévez, R., 2020. Megalencephalic leukoencephalopathy: insights into pathophysiology and perspectives for therapy. Front. Cell. Neurosci. 14, 627887 https://doi.org/10.3389/fncel.2020.627887.

Bosch, M.E., Kielian, T., 2019. Astrocytes in juvenile neuronal ceroid lipofuscinosis (CLN3) display metabolic and calcium signaling abnormalities. J. Neurochem. 148, 612–624. https://doi.org/10.1111/jnc.14545.

Brignone, M.S., Lanciotti, A., Macioce, P., Macchia, G., Gaetani, M., Aloisi, F., Petrucci, T. C., Ambrosini, E., 2011. The β1 subunit of the Na,K-ATPase pump interacts with megalencephalic leucoencephalopathy with subcortical cysts protein 1 (MLC1) in brain astrocytes: new insights into MLC pathogenesis. Hum. Mol. Genet. 20, 90–103. https://doi.org/10.1093/hmg/ddq435.

Brignone, M.S., Lanciotti, A., Visentin, S., De Nuccio, C., Molinari, P., Camerini, S., Diociaiuti, M., Petrini, S., Minnone, G., Crescenzi, M., Laudiero, L.B., Bertini, E., Petrucci, T.C., Ambrosini, E., 2014. Megalencephalic leukoencephalopathy with subcortical cysts protein-1 modulates endosomal pH and protein trafficking in astrocytes: relevance to MLC disease pathogenesis. Neurobiol. Dis. 66, 1–18. https://doi.org/10.1016/j.nbd.2014.02.003.

Brignone, M.S., Lanciotti, A., Camerini, S., De Nuccio, C., Petrucci, T.C., Visentin, S., Ambrosini, E., 2015. MLC1 protein: a likely link between leukodystrophies and brain channelopathies. Front. Cell. Neurosci. 9, 66. https://doi.org/10.3389/fncel.2015.00106.

Brignone, M.S., Lanciotti, A., Serafini, B., Mallozzi, C., Sbriccoli, M., Veroni, C., Molinari, P., Elorza-Vidal, X., Petrucci, T.C., Estévez, R., Ambrosini, E., 2019. Megalencephalic leukoencephalopathy with subcortical cysts Protein-1 (MLC1) counteracts astrocyte activation in response to inflammatory signals. Mol. Neurobiol. 56, 8237–8254. https://doi.org/10.1007/s12035-019-01657-y.

Brignone, M.S., Lanciotti, A., Michelucci, A., Mallozzi, C., Camerini, S., Catacuzzeno, L., Sforna, L., Caramia, M., D'Adamo, M.C., Ceccarini, M., Molinari, P., Macioce, P., Macchia, G., Petrucci, T.C., Pessia, M., Visentin, S., Ambrosini, E., 2022. The CaMKII/MLC1 Axis confers Ca2+-dependence to volume-regulated anion channels (VRAC) in astrocytes. Cells 11, 2656. https://doi.org/10.3390/cells11172656.

Bugiani, M., Dubey, M., Breur, M., Postma, N.L., Dekker, M.P., Ter Braak, T., Boschert, U., Abbink, T.E.M., Mansvelder, H.D., Min, R., Van Weering, J.R.T., Van Der Knaap, M.S., 2017. Megalencephalic leukoencephalopathy with cysts: the Glialcam -null mouse model. Ann. Clin. Transl. Neurol. 4, 450–465. https://doi.org/10.1002/acn3.405.

Calogero, A., Lombari, V., De Gregorio, G., Porcellini, A., Ucci, S., Arcella, A., Caruso, R., Gagliardi, F.M., Gulino, A., Lanzetta, G., Frati, L., Mercola, D., Ragona, G., 2004. Inhibition of cell growth by EGR-1 in human primary cultures from malignant glioma. Cancer Cell Int. 4, 1. https://doi.org/10.1186/1475-2867-4-1.

Capdevila-Nortes, X., López-Hernández, T., Apaja, P.M., López De Heredia, M., Sirisi, S., Callejo, G., Arnedo, T., Nunes, V., Lukacs, G.L., Gasull, X., Estévez, R., 2013. Insights into MLC pathogenesis: GlialCAM is an MLC1 chaperone required for proper activation of volume-regulated anion currents. Hum. Mol. Genet. 22, 4405–4416. https://doi.org/10.1093/hmg/ddt290.

Dai, H., Song, D., Xu, J., Li, B., Hertz, L., Peng, L., 2013. Ammonia-induced Na,K-ATPase/ouabain-mediated EGF receptor transactivation, MAPK/ERK and PI3K/AKT signaling and ROS formation cause astrocyte swelling. Neurochem. Int. 63, 610–625. https://doi.org/10.1016/j.neuint.2013.09.005.

Denizot, A., Arizono, M., Nägerl, U.V., Soula, H., Berry, H., 2019. Simulation of calcium signaling in fine astrocytic processes: effect of spatial properties on spontaneous activity. PLoS Comput. Biol. 15, e1006795 https://doi.org/10.1371/journal.pcbi.1006795.

Duarri, A., Lopez De Heredia, M., Capdevila-Nortes, X., Ridder, M.C., Montolio, M., López-Hernández, T., Boor, I., Lien, C.-F., Hagemann, T., Messing, A., Gorecki, D.C., Scheper, G.C., Martínez, A., Nunes, V., Van Der Knaap, M.S., Estévez, R., 2011. Knockdown of MLC1 in primary astrocytes causes cell vacuolation: a MLC disease cell model. Neurobiol. Dis. 43, 228–238. https://doi.org/10.1016/j.nbd.2011.03.015.

Eilert-Olsen, M., Hjukse, J.B., Thoren, A.E., Tang, W., Enger, R., Jensen, V., Pettersen, K. H., Nagelhus, E.A., 2019. Astroglial endfeet exhibit distinct Ca 2+ signals during hypoosmotic conditions. Glia 67, 2399–2409. https://doi.org/10.1002/glia.23692.

Eleuteri, C., Olla, S., Veroni, C., Umeton, R., Mechelli, R., Romano, S., Buscarinu, Mc, Ferrari, F., Calò, G., Ristori, G., Salvetti, M., Agresti, C., 2017. A staged screening of registered drugs highlights remyelinating drug candidates for clinical trials. Sci. Rep. 7, 45780. https://doi.org/10.1038/srep45780.

Elorza-Vidal, X., Sirisi, S., Gaitán-Peñas, H., Pérez-Rius, C., Alonso-Gardón, M., Armand-Ugón, M., Lanciotti, A., Brignone, M.S., Prat, E., Nunes, V., Ambrosini, E., Gasull, X., Estévez, R., 2018. GlialCAM/MLC1 modulates LRRC8/VRAC currents in an indirect manner: implications for megalencephalic leukoencephalopathy. Neurobiol. Dis. 119, 88–99. https://doi.org/10.1016/j.nbd.2018.07.031.

Etxeberria, A., Aivar, P., Rodriguez-Alfaro, J.A., Alaimo, A., Villace, P., Gomez-Posada, J. C., Areso, P., Villarroel, A., 2008. Calmodulin regulates the trafficking of KCNQ2 potassium channels. FASEB J. 22, 1135–1143. https://doi.org/10.1096/fj.07-9712com.

Fischer, R., Schliess, F., Häussinger, D., 1997. Characterization of the hypo-osmolarity-induced Ca2+ response in cultured rat astrocytes. Glia 20, 51–58.

Fujii, Y., Maekawa, S., Morita, M., 2017. Astrocyte calcium waves propagate proximally by gap junction and distally by extracellular diffusion of ATP released from volume-regulated anion channels. Sci. Rep. 7, 13115. https://doi.org/10.1038/s41598-017-13243-0.

Gilbert, A., Elorza-Vidal, X., Rancillac, A., Chagnot, A., Yetim, M., Hingot, V., Deffieux, T., Boulay, A.-C., Alvear-Perez, R., Cisternino, S., Martin, S., Taïb, S., Gelot, A., Mignon, V., Favier, M., Brunet, I., Declèves, X., Tanter, M., Estevez, R., Vivien, D., Saubaméa, B., Cohen-Salmon, M., 2021. Megalencephalic leukoencephalopathy with subcortical cysts is a developmental disorder of the gliovascular unit. eLife 10, e71379. https://doi.org/10.7554/eLife.71379.

Hamilton, E.M.C., Tekturk, P., Cialdella, F., Van Rappard, D.F., Wolf, N.I., Yalcinkaya, C., Çetinçelik, Ü., Rajaee, A., Kariminejad, A., Paprocka, J., Yapici, Z., Bošnjak, V.M., Van Der Knaap, M.S., 2018. Megalencephalic leukoencephalopathy with subcortical cysts: characterization of disease variants. Neurology 90, e1395–e1403. https://doi.org/10.1212/WNL.0000000000005334.

Hoegg-Beiler, M.B., Sirisi, S., Orozco, I.J., Ferrer, I., Hohensee, S., Auberson, M., Gödde, K., Vilches, C., De Heredia, M.L., Nunes, V., Estévez, R., Jentsch, T.J., 2014. Disrupting MLC1 and GlialCAM and ClC-2 interactions in leukodystrophy entails glial chloride channel dysfunction. Nat. Commun. 5, 3475. https://doi.org/10.1038/ncomms4475.

Joiner, W.J., Khanna, R., Schlichter, L.C., Kaczmarek, L.K., 2001. Calmodulin regulates assembly and trafficking of SK4/IK1 Ca2+−activated K+ channels. J. Biol. Chem. 276, 37980–37985. https://doi.org/10.1074/jbc.M104965200.

Koizumi, S., Shigetomi, E., Sano, F., Saito, K., Kim, S.K., Nabekura, J., 2021. Abnormal Ca2+ signals in reactive astrocytes as a common cause of brain diseases. IJMS 23, 149. https://doi.org/10.3390/ijms23010149.

Kovacs, G.G., Zsembery, A., Anderson, S.J., Komlosi, P., Gillespie, G.Y., Bell, P.D., Benos, D.J., Fuller, C.M., 2005. Changes in intracellular Ca 2+ and pH in response to thapsigargin in human glioblastoma cells and normal astrocytes. American Journal of Physiology-Cell Physiology 289, C361–C371. https://doi.org/10.1152/ajpcell.00280.2004.

Kovalevskaya, N.V., Van De Waterbeemd, M., Bokhovchuk, F.M., Bate, N., Bindels, R.J. M., Hoenderop, J.G.J., Vuister, G.W., 2013. Structural analysis of calmodulin binding to ion channels demonstrates the role of its plasticity in regulation. Pflugers Arch. - Eur. J. Physiol. 465, 1507–1519. https://doi.org/10.1007/s00424-013-1278-0.

Lanciotti, A., Brignone, M.S., Camerini, S., Serafini, B., Macchia, G., Raggi, C., Molinari, P., Crescenzi, M., Musumeci, M., Sargiacomo, M., Aloisi, F., Petrucci, T.C., Ambrosini, E., 2010. MLC1 trafficking and membrane expression in astrocytes: role of caveolin-1 and phosphorylation. Neurobiol. Dis. 37, 581–595. https://doi.org/10.1016/j.nbd.2009.11.008.

Lanciotti, A., Brignone, M.S., Molinari, P., Visentin, S., De Nuccio, C., Macchia, G., Aiello, C., Bertini, E., Aloisi, F., Petrucci, T.C., Ambrosini, E., 2012. Megalencephalic leukoencephalopathy with subcortical cysts protein 1 functionally cooperates with the TRPV4 cation channel to activate the response of astrocytes to osmotic stress: dysregulation by pathological mutations. Hum. Mol. Genet. 21, 2166–2180. https://doi.org/10.1093/hmg/dds032.

Lanciotti, A., Brignone, M.S., Visentin, S., De Nuccio, C., Catacuzzeno, L., Mallozzi, C., Petrini, S., Caramia, M., Veroni, C., Minnone, G., Bernardo, A., Franciolini, F., Pessia, M., Bertini, E., Petrucci, T.C., Ambrosini, E., 2016. Megalencephalic leukoencephalopathy with subcortical cysts protein-1 regulates epidermal growth factor receptor signaling in astrocytes. Hum. Mol. Genet. 25, 1543–1558. https://doi.org/10.1093/hmg/ddw032.

Lanciotti, A., Brignone, M.S., Belfiore, M., Columba-Cabezas, S., Mallozzi, C., Vincentini, O., Molinari, P., Petrucci, T.C., Visentin, S., Ambrosini, E., 2020. Megalencephalic leukoencephalopathy with subcortical cysts disease-linked MLC1 protein favors gap-junction intercellular communication by regulating Connexin 43 trafficking in astrocytes. Cells 9, 1425. https://doi.org/10.3390/cells9061425.

Lee, J.H., Lee, J., Choi, K.Y., Hepp, R., Lee, J.-Y., Lim, M.K., Chatani-Hinze, M., Roche, P. A., Kim, D.G., Ahn, Y.S., Kim, C.H., Roche, K.W., 2008. Calmodulin dynamically regulates the trafficking of the metabotropic glutamate receptor mGluR5. Proc. Natl. Acad. Sci. U. S. A. 105, 12575–12580. https://doi.org/10.1073/pnas.0712033105.

Leegwater, P.A.J., Yuan, B.Q., Van Der Steen, J., Mulders, J., Könst, A.A.M., Boor, P.K.I., Mejaski-Bosnjak, V., Van Der Maarel, S.M., Frants, R.R., Oudejans, C.B.M., Schutgens, R.B.H., Pronk, J.C., Van Der Knaap, M.S., 2001. Mutations of MLC1 (KIAA0027), encoding a putative membrane protein, cause megalencephalic leukoencephalopathy with subcortical cysts. The American Journal of Human Genetics 68, 831–838. https://doi.org/10.1086/319519.

Leventoux, N., Augustus, M., Azar, S., Riquier, S., Villemin, J.P., Guelfi, S., Falha, L., Bauchet, L., Gozé, C., Ritchie, W., Commes, T., Duffau, H., Rigau, V., Hugnot, J.P., 2020. Transformation foci in IDH1-mutated gliomas show STAT3 phosphorylation and downregulate the metabolic enzyme ETNPPL, a negative regulator of glioma growth. Sci. Rep. 10, 5504. https://doi.org/10.1038/s41598-020-62145-1.

Liang, M., Tian, J., Liu, L., Pierre, S., Liu, J., Shapiro, J., Xie, Z.-J., 2007. Identification of a pool of non-pumping Na/K-ATPase. J. Biol. Chem. 282, 10585–10593. https://doi.org/10.1074/jbc.M609181200.

Lim, D., Semyanov, A., Genazzani, A., Verkhratsky, A., 2021. Calcium signaling in neuroglia. Int. Rev. Cell Mol. Biol. 362, 1–53. https://doi.org/10.1016/bs.ircmb.2021.01.003.

López-Hernández, T., Ridder, M.C., Montolio, M., Capdevila-Nortes, X., Polder, E., Sirisi, S., Duarri, A., Schulte, U., Fakler, B., Nunes, V., Scheper, G.C., Martínez, A., Estévez, R., van der Knaap, M.S., 2011. Mutant GlialCAM causes megalencephalic leukoencephalopathy with subcortical cysts, benign familial macrocephaly, and macrocephaly with retardation and autism. Am. J. Hum. Genet. 88, 422–432. https://doi.org/10.1016/j.ajhg.2011.02.009.

Moh, M.C., Lee, L.H., Zhang, T., Shen, S., 2009. Interaction of the immunoglobulin-like cell adhesion molecule hepaCAM with caveolin-1. Biochem. Biophys. Res. Commun. 378, 755–760. https://doi.org/10.1016/j.bbrc.2008.11.119.

Nighot, P.K., Blikslager, A.T., 2012. Chloride channel ClC-2 modulates tight junction barrier function via intracellular trafficking of occludin. Am. J. Phys. Cell Phys. 302, C178–C187. https://doi.org/10.1152/ajpcell.00072.2011.

Noël, G., Tham, D.K.L., Moukhles, H., 2009. Interdependence of laminin-mediated clustering of lipid rafts and the dystrophin complex in astrocytes. J. Biol. Chem. 284, 19694–19704. https://doi.org/10.1074/jbc.M109.010090.

O'Day, D.H., Huber, R.J., 2022. Calmodulin binding proteins and neuroinflammation in multiple neurodegenerative diseases. BMC Neurosci. 23, 10. https://doi.org/10.1186/s12868-022-00695-y.

Okubo, Y., 2020. Astrocytic Ca2+ signaling mediated by the endoplasmic reticulum in health and disease. J. Pharmacol. Sci. 144, 83–88. https://doi.org/10.1016/j.jphs.2020.07.006.

Pani, B., Singh, B.B., 2009. Lipid rafts/caveolae as microdomains of calcium signaling. Cell Calcium 45, 625–633. https://doi.org/10.1016/j.ceca.2009.02.009.

Pascual-Castroviejo, I., van der Knaap, M.S., Pronk, J.C., García-Segura, J.M., Gutiérrez-Molina, M., Pascual-Pascual, S.I., 2005. Vacuolating megalencephalic leukoencephalopathy: 24 year follow-up of two siblings. Neurologia 20, 33–40.

Passchier, E.M.J., Kerst, S., Brouwers, E., Hamilton, E.M.C., Bisseling, Q., Bugiani, M., Waisfisz, Q., Kitchen, P., Unger, L., Breur, M., Hoogterp, L., de Vries, S.I., Abbink, T. E.M., Kole, M.H.P., Leurs, R., Vischer, H.F., Brignone, M.S., Ambrosini, E., Feillet, F., Born, A.P., Epstein, L.G., Mansvelder, H.D., Min, R., van der Knaap, M.S., 2023. Aquaporin-4 and GPRC5B: old and new players in controlling brain oedema. Brain. https://doi.org/10.1093/brain/awad146 awad146.

Petrini, S., Minnone, G., Coccetti, M., Frank, C., Aiello, C., Cutarelli, A., Ambrosini, E., Lanciotti, A., Brignone, M.S., D'Oria, V., Strippoli, R., De Benedetti, F., Bertini, E., Bracci-Laudiero, L., 2013. Monocytes and macrophages as biomarkers for the diagnosis of megalencephalic leukoencephalopathy with subcortical cysts. Mol. Cell. Neurosci. 56, 307–321. https://doi.org/10.1016/j.mcn.2013.07.001.

Pizzo, P., Burgo, A., Pozzan, T., Fasolato, C., 2001 Oct. Role of capacitative calcium entry on glutamate-induced calcium influx in type-I rat cortical astrocytes. J Neurochem 79 (1), 98–109. https://doi.org/10.1046/j.1471-4159.2001.00539.x. PMID: 11595762.

Rezola, M., Castellanos, A., Gasull, X., Comes, N., 2021. Functional interaction between Caveolin 1 and LRRC8-mediated volume-regulated Anion Channel. Front. Physiol. 12, 691045 https://doi.org/10.3389/fphys.2021.691045.

Ridder, M.C., Boor, I., Lodder, J.C., Postma, N.L., Capdevila-Nortes, X., Duarri, A., Brussaard, A.B., Estévez, R., Scheper, G.C., Mansvelder, H.D., Van Der Knaap, M.S., 2011. Megalencephalic leucoencephalopathy with cysts: defect in chloride currents and cell volume regulation. Brain 134, 3342–3354. https://doi.org/10.1093/brain/awr255.

Roig, S.R., Solé, L., Cassinelli, S., Colomer-Molera, M., Sastre, D., Serrano-Novillo, C., Serrano-Albarrás, A., Lillo, M.P., Tamkun, M.M., Felipe, A., 2021. Calmodulin-dependent KCNE4 dimerization controls membrane targeting. Sci. Rep. 11, 14046. https://doi.org/10.1038/s41598-021-93562-5.

Roncarati, R., Decimo, I., Fumagalli, G., 2005. Assembly and trafficking of human small conductance Ca2+−activated K+ channel SK3 are governed by different molecular domains. Mol. Cell. Neurosci. 28, 314–325. https://doi.org/10.1016/j.mcn.2004.09.015.

Saito, K., Shigetomi, E., Yasuda, R., Sato, R., Nakano, M., Tashiro, K., Tanaka, K.F., Ikenaka, K., Mikoshiba, K., Mizuta, I., Yoshida, T., Nakagawa, M., Mizuno, T., Koizumi, S., 2018. Aberrant astrocyte Ca2+ signals "AxCa signals" exacerbate pathological alterations in an Alexander disease model. Glia 66, 1053–1067. https://doi.org/10.1002/glia.23300.

Sharma, P., Ghavami, S., Stelmack, G.L., McNeill, K.D., Mutawe, M.M., Klonisch, T., Unruh, H., Halayko, A.J., 2010. β-Dystroglycan binds caveolin-1 in smooth muscle: a functional role in caveolae distribution and Ca2+ release. J. Cell Sci. 123, 3061–3070. https://doi.org/10.1242/jcs.066712.

Shematorova, E.K., Shpakovski, D.G., Chernysheva, A.D., Shpakovski, G.V., 2018. Molecular mechanisms of the juvenile form of batten disease: important role of MAPK signaling pathways (ERK1/ERK2, JNK and p38) in pathogenesis of the malady. Biol. Direct 13, 19. https://doi.org/10.1186/s13062-018-0212-y.

Shigetomi, E., Saito, K., Sano, F., Koizumi, S., 2019. Aberrant calcium signals in reactive astrocytes: a key process in neurological disorders. IJMS 20, 996. https://doi.org/10.3390/ijms20040996.

Stokum, J.A., Shim, B., Negoita, S., Tsymbalyuk, N., Tsymbalyuk, O., Ivanova, S., Keledjian, K., Bryan, J., Blaustein, M.P., Jha, R.M., Kahle, K.T., Gerzanich, V., Simard, J.M., 2023. Cation flux through SUR1-TRPM4 and NCX1 in astrocyte endfeet induces water influx through AQP4 and brain swelling after ischemic stroke. Sci. Signal. 16, eadd6364. https://doi.org/10.1126/scisignal.add6364.

Sunagawa, M., Yokoshiki, H., Seki, T., Nakamura, M., Laber, P., Sperelakis, N., 1999. Direct block of Ca2+ channels by Calmidazolium in cultured vascular smooth muscle cells. J. Cardiovasc. Pharmacol. 34, 488–496. https://doi.org/10.1097/00005344-199910000-00003.

Swulius, M.T., Waxham, M.N., 2008. Ca2+/Calmodulin-dependent Protein Kinases. Cell. Mol. Life Sci. 65, 2637–2657. https://doi.org/10.1007/s00018-008-8086-2.

Teijido, O., Martínez, A., Pusch, M., Zorzano, A., Soriano, E., Del Río, J.A., Palacín, M., Estévez, R., 2004. Localization and functional analyses of the MLC1 protein involved in megalencephalic leukoencephalopathy with subcortical cysts. Hum. Mol. Genet. 13, 2581–2594. https://doi.org/10.1093/hmg/ddh291.

Topçu, M., Gartioux, C., Ribierre, F., Yalçinkaya, C., Tokus, E., Öztekin, N., Beckmann, J. S., Ozguc, M., Seboun, E., 2000. Vacuoliting megalencephalic leukoencephalopathy with subcortical cysts, mapped to chromosome 22qtel. Am. J. Hum. Genet. 66, 733–739. https://doi.org/10.1086/302758.

Urrutia, J., Aguado, A., Muguruza-Montero, A., Núñez, E., Malo, C., Casis, O., Villarroel, A., 2019. The crossroad of ion channels and calmodulin in disease. IJMS 20, 400. https://doi.org/10.3390/ijms20020400.

Van Der Knaap, M.S., Barth, P.G., Vrensen, G.F.J.M., Valk, J., 1996. Histopathology of an infantile-onset spongiform leukoencephalopathy with a discrepantly mild clinical course. Acta Neuropathol. 92, 206–212. https://doi.org/10.1007/s004010050510.

Verkhratsky, A., 2006. Glial calcium signaling in physiology and pathophysiology1. Acta Pharmacol. Sin. 27, 773–780. https://doi.org/10.1111/j.1745-7254.2006.00396.x.

Walch, E., Fiacco, T.A., 2022. Honey, I shrunk the extracellular space: measurements and mechanisms of astrocyte swelling. Glia 70, 2013–2031. https://doi.org/10.1002/glia.24224.

Weerth, S.H., Holtzclaw, L.A., Russell, J.T., 2007. Signaling proteins in raft-like microdomains are essential for Ca2+ wave propagation in glial cells. Cell Calcium 41, 155–167. https://doi.org/10.1016/j.ceca.2006.06.006.

Yaduvanshi, S., Ero, R., Kumar, V., 2021. The mechanism of complex formation between calmodulin and voltage gated calcium channels revealed by molecular dynamics. PloS One 16, e0258112. https://doi.org/10.1371/journal.pone.0258112.

Zamora, N.N., Cheli, V.T., Santiago González, D.A., Wan, R., Paez, P.M., 2020. Deletion of voltage-gated calcium channels in astrocytes during demyelination reduces brain inflammation and promotes myelin regeneration in mice. J. Neurosci. 40, 3332–3347. https://doi.org/10.1523/JNEUROSCI.1644-19.2020.

Zhu, A., Lin, Yao, Hu, X., Lin, Z., Lin, Yongqiang, Xie, Q., Ni, S., Cheng, H., Lu, Q., Lai, S., Pan, G., Chen, X., Pang, W., Liu, C., 2022. Treadmill exercise decreases cerebral edema in rats with local cerebral infarction by modulating AQP4 polar expression through the caveolin-1/TRPV4 signaling pathway. Brain Res. Bull. 188, 155–168. https://doi.org/10.1016/j.brainresbull.2022.08.003.